Beitr. Paläont., **31**:157–187, Wien 2009

The Late Miocene Mammal Faunas of the Mytilinii Basin, Samos Island, Greece: New Collection

9. Rhinocerotidae

by

Ioannis X. Giaourtsakis[*)]

Giaourtsakis, I.X., 2009. The Late Miocene Mammal Faunas of the Mytilinii Basin, Samos Island, Greece: New Collection. 9. Rhinocerotidae. — Beitr. Paläont., **31**:157–187, Wien.

Abstract

The recent paleontological expeditions to the late Miocene fossiliferous localities of the Mytilinii Basin on Samos Island, Greece, have unearthed numerous rhinocerotid remains that represent two species of horned rhinoceroses, "*Diceros*" *neumayri* (Osborn, 1900) and *Dihoplus pikermiensis* (Toula, 1906). The morphological differences between the two species are discussed. The absence of the hornless rhinoceros *Chilotherium* in our sample, which is known from previous Samos collections, is attributed to the limited material, particularly from the stratigraphically older localities of Mytilinii-3 (MYT) and Mytilinii-4 (MLN) of the Potamies ravine. In the well-sampled localities of the younger Mytilinii-1 (MTL) faunal assemblage of the Adrianos ravine, a significant interspecific dominance of "*Diceros*" *neumayri* over *Dihoplus pikermiensis* has been documented. The comparison of the Samos rhinocerotids with other Turolian localities in Continental Greece and Western Asia indicates a closer resemblance to the Asian ones, in particular from Anatolia. The marked differences in the relative distribution of rhinocerotid taxa among the Turolian localities of the Eastern Mediterranean and adjacent regions are related to environmentally-controlled provincial differences and suggest the expansion of more open and arid habitats on Samos and in Anatolia compared to Continental Greece during this period of time.

Keywords: Turolian, Samos, Greece, Mammalia, Perissodactyla, Rhinocerotidae, Systematics.

Zusammenfassung

Die jüngsten paläontologischen Forschungen in den obermiozänen Fossilfundstellen des Mytilinii Beckens (Samos, Griechenland), haben zahlreiche Nashornreste erbracht, die zwei verschiedene horntragende Nashornarten beinhalten: "*Diceros*" *neumayri* (Osborn, 1900) und *Dihoplus pikermiensis* (Toula, 1906). Die morphologischen Unterschiede zwischen den zwei Arten werden besprochen. Das Fehlen des hornlosen Nashorns *Chilotherium*, das aus früheren Ausgrabungen auf Samos bekannt ist, hängt möglicherweise mit dem begrenzten Fundmaterial zusammen, insbesondere aus den stratigraphisch älteren Fundstellen Mytilinii-3 (MYT) und Mytilinii-4 (MLN) der Potamies Schlucht. In den fossilreichen und stratigraphisch jüngeren Fundstellen Mytilinii-1 (MTL) der Andrianos Schlucht ist eine klare interspezifische Dominanz von "*Diceros*" *neumayri* über *Dihoplus pikermiensis* dokumentiert worden. Der Vergleich der Nashornfauna von Samos mit anderen turolischen Fundstellen aus dem kontinentalen Griechenland und aus West-Asien zeigt eine stärkere Ähnlichkeit mit den asiatischen Fundstellen, insbesondere jenen aus Anatolien. Die markanten Unterschiede in der relativen Verteilung der verschiedenen Nashornarten in den turolischen Fundstellen im östlichen Mittelmeerraum und in den benachbarten Regionen hängen mit klimatischen provinziellen Unterschieden zusammen. Sie deuten die Verbreitung von offeneren und trockeneren Lebensräumen auf Samos und in Anatolien während des Turoliums an, im Vergleich zu den Fundstellen des kontinentalen Griechenlands.

Schlüsselwörter: Turolium, Samos, Griechenland, Mammalia, Perissodactyla, Rhinocerotidae, Systematik.

1. Introduction

The presence of fossil mammals on Samos Island has been known since early historical times, as indicated by surviving ancient Greek myths and artifacts (Solounias

---

[*)] Dipl.-Geol. Ioannis X. Giaourtsakis, Ludwig-Maximilians-University of Munich, Department of Geo- and Environmental Sciences, Section of Paleontology. Richard-Wagner-Str. 10, D-80333 Munich, Germany. e-mail: i.giaourtsakis@lrz.uni-muenchen.de

& Mayor, 2004; Koufos, this volume). The first documented rhinocerotid fossils from Samos were part of a small collection collected by local villagers that was sold to Italian travelers sometime between 1852 and 1866. These specimens were deposited at the Geological Institute of the University of Padova and were reported much later by Leonardi (1947) and Piccoli et al. (1975). The first systematic excavations on Samos were conducted during the years 1885-1889 by the English physician and naturalist C. I. Forsyth Major, who was inspired by the ancient myths (Forsyth-Major, 1888, 1891, 1994). In the catalog of his major findings, Forsyth-Major (1894) attributed several rhinocerotid specimens to *Rhinoceros pachygnathus* (here *"Diceros" neumayri*), a well-known species at that time from the renowned locality of Pikermi (Wagner, 1848; Gaudry, 1863). Following the impressive discoveries of Forsyth Major, a great number of expeditions was carried out on Samos by a variety of fossil dealers and scientists during the next decades, spreading the amply recovered material to numerous museums and institutional collections across Europe and the USA (Solounias, 1981a, b; Koufos, this volume).

The first detailed studies on the Samos rhinoceroses were undertaken by Weber (1904, 1905), who described and illustrated a remarkably rich collection hosted at that time at the Paleontological Museum of Munich. In his first contribution, Weber (1904) studied the remains of the horned rhinoceroses (subfamily Rhinocerotinae). Apart from the dominant *Rhinoceros pachygnathus* (here *"Diceros" neumayri*), Weber also recognized the presence of a second horned rhinoceros species on Samos, which he referred to *Rhinoceros schleiermacheri* (here attributed to *Dihoplus pikermiensis*). In his second contribution, Weber (1905) documented the presence of two additional hornless rhinoceros species (subfamily Aceratherinae), which he attributed to the new species *Aceratherium schlosseri* and *Aceratherium samium*. Later on, both hornless species were properly included by Ringström (1924) in his newly created genus *Chilotherium*. Unfortunately, the entire rhinocerid material from Samos at Munich was destroyed by a heavy bombing during the Second World War. A second systematic study was undertaken by Andreé (1921), who examined the Samos rhinocerotid collection at the Paleontological Museum of Münster. Andreé (1921) recognized the four species previously documented by Weber (1904, 1905), and created two additional hornless rhinoceros species, *Aceratherium wegneri* and *Aceratherium angustifrons*. However, their specific identity is doubtful. The rather well-preserved type cranium with associated mandible of *Aceratherium wegneri* evidently belongs to Weber's *Chilotherium schlosseri*, as first suggested by Heissig (1975a, b). The incomplete and transversally compressed type cranium of *Aceratherium angustifrons* may either belong to *Chilotherium kowalevskii* (Pavlow, 1913), as indicated by Heissig (1975a, b), or perhaps it may also represent Weber's *Chilotherium schlosseri*. Unfortunately, its type cranium is currently considered lost (Meiburg & Siegfried, 1970), so that no safe conclusions can be reached. During the subsequent decades, some impressive rhinocerotid skulls from Samos were depicted and briefly described in short accounts on the Samos fauna accumulated in various Museums (Drevermann, 1930; Leonardi, 1947; Melentis, 1968; Piccoli et al., 1975; Lehmann, 1984), or in general works (Thenius, 1955; Viret, 1958). Geraads (1988) presented a significant study on the horned rhinoceros species from Pikermi and Samos, establishing reliable criteria for distinguishing the cranial and dental remains of *"Diceros" neumayri* and *Dihoplus pikermiensis*. Giaourtsakis et al. (2006) refined the morphological differences of their mandibles and deciduous dentitions, and discussed their relative distribution and interspecific dominance in Pikermi and on Samos.

In the present study, we describe the rhinocerotid material collected during the recent paleontological expeditions on Samos that were conducted under the direction of Prof. G.D. Koufos, under the auspices of the "K. and M. Zimalis Foundation" and the Aegean Museum of Natural History (Koufos, this volume). The studied material was unearthed from three localities, Mytilinii-4 (MLN), Mytilinii-3 (MYT), and Mytilinii-1 (MTL). The locality MLN is placed in the Potamies ravine and is dated to early Turolian (uppermost MN 11) at ~7.5 Ma. The locality MYT is situated in the Potamies ravine and is dated to early middle Turolian (early MN 12) at ~7.3 Ma. The locality MTL is located in Adrianos ravine and consists of several fossiliferous sites; the rhinocerotids have been traced in the sites MTLA, MTLB, MTLD dated to the uppermost middle Turolian (MN 12) at ~7.1 Ma. Further, the specimens from the 1963 expedition by Prof. J.K. Melentis in Adrianos ravine (Melentis, 1968) are also included in the present study. Melentis' excavation site coincides with Mytilinii-1A (MTLA), but to avoid confusion, the specimens of this collection are referred to by the prefix PMMS before their code number (Koufos, this volume). A detailed account on the geological and stratigraphical setting of the different fossiliferous sites of Samos is provided by Kostopoulos et al. (this volume) and Koufos et al. (this volume-a).

2. Material and Methods

The rhinocerotid material described in the present article is stored in the collections of the Natural History Museum of the Aegean, Mytilinii, Samos (NHMA). Cranial and mandibular measurements follow Guérin (1980), including a few additional measurements. Anatomical conventions follow Getty (1975) and Baron (1999), also considering the recommendations of NAV (2005). Dental measurements and terminology follow Peter (2002), but width measurements include the mesial (Wm), as well as the distal (Wd) width of each tooth. On the first upper and lower deciduous premolar, only the maximal distal width (Wd) is measured. Measurements of M3 include the buccal length of the ectometaloph (Lb), the mesial width (Wm) and the lingual, anatomical length (La), comprising the distal cingular pillar, if present (Peter, 2002; Guérin, 1980). Measurements ranging from 0-150 mm were taken with a digital caliper to 0.01 mm and rounded to the nearest 0.1 mm. For larger measurements a linear caliper with a precision of 0.1 mm was applied. All measurements are given in millimeters (mm).

Comparative studies with material from Greece (Pikermi, Samos, Kerassia, Halmyropotamos, Axios Valley: Wagner, 1848; Gaudry, 1863; Arambourg & Piveteau, 1929; Melentis, 1967, 1969; Koufos, 1980; Geraads, 1988; Geraads & Koufos, 1990; Giaourtsakis, 2003; Giaourtsakis et al., 2006) were carried out in the collections of the AMPG, LGPUT, MNHN, BMNH, NHMW, IPUW, MAFI, BSPG, NHMB, HLMD, SMF, and SMNS; those from Turkey (various localities: Heissig, 1975, 1996; Geraads, 1994; Fortelius et al., 2003; Antoine & Saraç, 2005) were studied at the BSPG, SMNK, and MNHN; and those from Iran (Maragheh: Osborn, 1900; Thenius, 1955) at the NHMW, MNHN, and BMNH. Rhinocerotid material from other key Neogene Eurasian and African localities was also examined at the collections of the aforementioned museums and institutes. Comparative studies with the extant species were carried out at the zoological collections of the BMNH, MNHN, NHMW, RMNH, ZMA, ZSM, SMNK, SMNS, SMF, and ZMUC.

Institutional Abbreviations:

AMNH: American Museum of Natural History, New York; AMPG: Athens Museum of Paleontology and Geology, University of Athens; BMNH: British Museum of Natural History (=Natural History Museum), London; BSPG: Bayerische Staatssammlung für Paläontologie und Geologie, München; GPMM: Geologisch-Paläontologisches Museum der Universität Münster; GPMH: Geologisch-Paläontologisches Museum der Universität Hamburg; HLMD: Hessisches Landesmuseum, Darmstadt; IPUW: Institut für Paläontologie der Universität Wien; LGPUT: Laboratory of Geology and Palaeontology, University of Thessaloniki; MAFI: Magyar Állami Földtani Intézet, Budapest; MCGL: Musée Cantonal de Géologie, Lausanne; MGPP: Museo di Geologia e Paleontologia dell'Università di Padova; MNHB: Museum für Naturkunde der Humboldt Universität zu Berlin; MNHN: Muséum National d'Histoire Naturelle, Paris; NHMA: Natural History Museum of the Aegean, Mytilinii, Samos; NHMW: Naturhistorisches Museum, Wien; NME: National Museum of Ethiopia, Addis Ababa; RMNH: Rijkmuseum van Natuurlijke Historie (=Naturalis, Nationaal Natuurhistorisch Museum), Leiden; SMF: Forschungsinstitut und Naturmuseum Senckenberg, Frankfurt am Main; SMNK: Staatliches Museum für Naturkunde, Karlsruhe; SMNS: Staatliches Museum für Naturkunde, Stuttgart; ZMA: Zoologisch Museum, Universiteit van Amsterdam; ZMUC: Zoological Museum of the University of Copenhagen; ZSM: Zoologische Staatssammlung, München.

Morphological Abbreviations:

P, M, D: upper premolar, molar, deciduous molar; I, DI: upper incisor, deciduous incisor; p, m, d: lower premolar, molar, deciduous molar; i, di: lower incisor, deciduous incisor; MC: metacarpal; MT: metatarsal; dia.: diaphysis; ep.: epiphysis; prox.: proximal; dist.: distal; L: length; W: width; H: height; DT: transversal diameter; DAP: anteroposterior diameter; MNI: minimum number of individuals.

To avoid taxonomic confusion, only the extant species *Diceros bicornis* (*D. bicornis*) and *Ceratotherium simum* (*C. simum*) are abbreviated.

3. Taxonomic and Nomenclatural Notes

Extant horned rhinoceroses and their fossil relatives are commonly classified in three lineages: the rhinocerotines (includes extant *Rhinoceros unicornis* and *Rhinoceros sondaicus*), the dicerorhines (includes extant *Dicerorhinus sumatrensis*), and the dicerotines (includes extant *Diceros bicornis* and *Ceratotherium simum*). However, their phylogenetic relationships and suprageneric classification have been highly controversial, with numerous arrangements proposed and debated (Guérin, 1980, 1989; Heissig, 1981, 1989; Groves, 1983; Prothero et al., 1986; Geraads, 1988; Prothero & Schoch, 1989; Cerdeño, 1995; McKenna & Bell, 1997; Antoine, 2002). Even molecular studies on the five extant species have failed to resolve this trichotomy satisfactorily, also resulting in contradicting conclusions (Morales & Melnick, 1994; Tougard et al., 2001; Orlando et al., 2002; Hsing-Mei et al., 2003). They are considered here conditionally as three different tribes (Dicerotini Ringström, 1924; Rhinocerotini Owen, 1845; Dicerorhinini Ringström, 1924), forming together the subfamily Rhinocerotinae Owen, 1845, of the "true (modern) horned rhinoceroses" It is generally accepted that the radiation of the three lineages occurred early and rapidly in their evolutionary history, causing the existing difficulties and disagreements.

The occurrence of two different horned rhinoceros species during the Late Miocene in Greece has been recognized early on (Gaudry, 1863; Weber, 1904). However, both taxa suffer from some complex nomenclatural issues caused by frequent misidentifications and systematic discrepancies during the past (compare discussions in Kretzoi, 1942; Heissig, 1975; Geraads, 1988, 2005; Giaourtsakis, 2003, Giaourtsakis et al., 2006, in press). In the present study, the Dicerorhinini rhinoceros from Samos is attributed to *Dihoplus pikermiensis*, following Giaourtsakis (2003), whereas the Dicerotini rhinoceros from Samos is provisionally referred to as "*Diceros*" *neumayri*, following Giaourtsakis et al. (in press).

4. Systematic Paleontology

Order Perissodactyla Owen, 1848
Family Rhinocerotidae Owen, 1845
Subfamily Rhinocerotinae Owen, 1845
Tribe Dicerotini Ringström, 1924

Genus *Diceros* Gray, 1821

"Diceros" neumayri (Osborn, 1900)
(Plates 1-5)

Localities: Mytilinii-1A, B, D (MTLA, MTLB, MTLD), Adrianos ravine, Mytilinii Basin, Samos, Greece; Mytilinii-3 (MYT) and Mytilinii-4 (MLN), Potamies ravine, Mytilinii Basin, Samos, Greece.

Age: Turolian, late Miocene

Mytilinii-1A, B, D (MTLA, MTLB, MTLD): middle Turolian (MN 12), ~7.1 Ma

Mytilinii-3 (MYT): middle Turolian (early MN 12), ~7.3 Ma

Mytilinii-4 (MLN): early Turolian (uppermost MN 11), ~7.5 Ma

Material:

MTLA: Cranium with right P2-M3 and left P3-M3, MTLA-5; juvenile cranium with right D1-M1 and left D1-M1, MTLA-212; associated teeth: right M2-M3 and left P2, P3-P4, M1-M2, M3, MTLA-425; right P4?, MTLA-337; small maxillary fragment with left D2-D3, MTLA-27; small maxillary fragment with right D2-D3, MTLA-521; small maxillary fragment with left D2-D3, MTLA-98; left D1, MTLA-443; left D2, MTLA-497; mandibular fragment with right d1, d3-d4, MTLA-179; small mandibular fragment with left d3-d4, MTLA-242; small mandibular fragment with right d3-d4, MTLA-371; left d2, MTLA-239; right d2, MTLA-307; right scapula, MTLA-330; right humerus, MTLA-201; left humerus, MTLA-331; left radius and ulna, MTLA-177; left radius and ulna, MTLA-250; right radius and ulna, MTLA-340; right radius and ulna, MTLA-382; right radius and ulna, MTLA-531; left radius, MTLA-381; left ulna, MTLA-322; right ulna, MTLA-545; right scaphoid, MTLA-102; left pyramidal, MTLA-510; right unciforme, MTLA-101; right Mc-II, MTLA-99; right Mc-II, MTLA-388; right Mc-III and Mc-IV, MTLA-55; left Mc-III and Mc-IV, MTLA-289.A; left Mc-III, MTLA-123; right Mc-III, MTLA-24; right Mc-IV, MTLA-25; right femur, MTLA-124; left femur, MTLA-552; left femur, MTLA-553; left tibia and fibula, MTLA-251; right tibia, MTLA-321; left tibia, MTLA-533; right astragalus, MTLA-308; right calcaneus, MTLA-154; right Mt-II, MTLA-525; left Mt-III, MTLA-100; left Mt-III and Mt-IV, MTLA-289.B; left Mt-IV, MTLA-178.

MTLB: Juvenile partial cranium with right D2-M1 and left D1-M1, MTLB-43; adult cranial fragment, MTLB-339; adult cranial fragment, MTLB-340; left maxillary fragment with D1-D3, MTLB-87; right mandibular fragment with d4, MTLB-109; right humerus, MTLB-329; right humerus, MTLB-343; associated right elements: calcaneus, MTLB-19, cuboid, MTLB-20, Mt-III, MTLB-21, and Mt-IV, MTLB-22; right calcaneus, MTLB-248; right Mt-III and Mt-IV, MTLB-376.

MTLD: Right humerus, MTLD-1; left radius, MTLD-2; right Mc-III, MTLD-3; right Mc-III, MTLD-4; right Mc-IV, MTLD-5; right lunatum, MTLD-6; left astragalus, MTLD-7.

PMMS: Right femur, PMMS-48; right humerus, PMMS-58; right humerus, PMMS-60; left femur, PMMS-61; right femur, PMMS-66; atlas, PMMS-68; right Mt-IV, PMMS-73; left Mt-II, PMMS-74; associated right femur, tibia, fibula, PMMS-102; right femur, PMMS-105; mandible with right and left p2-m3, PMMS-106; cranium with right and left P4-M3, PMMS-107; mandible with right and left p2-m3, PMMS-108; left humerus, PMMS-109; right humerus, PMMS-112; right femur, PMMS-113; right tibia and fibula, PMMS-117; left trapezium, PMMS-238; left humerus, PMMS-1n; left calcaneus, PMMS-2n; right radius, PMMS-3n; right radius, PMMS-4n; left unciforme, PMMS-5n; left humerus, PMMS-6n; right humerus, PMMS-7n; right humerus, PMMS-8n.

MYT: Right radius, MYT-69; right scaphoid, MYT-61; right pyramidal, MYT-12; unnumbered right magnum, MYT-nn.

MLN: Left radius, MLN-41; right Mt-II, MLN-56.

Measurements: The measurements for the cranial and dental elements are provided in Tables 2-7.

"Diceros" neumayri is well-represented in our sample with a total number of 124 specimens and a minimum number of 22 individuals (Table 1). The material comprises cranial, dental, and postcranial specimens of both adult and juvenile individuals.

Adult Crania

The most prominent specimen is a nearly complete adult cranium, MTLA-5 (Pl. 1, fig.1; Pl. 2, fig. 1). Apart from the left zygomatic arch, which is compressed and mediodorsally elevated, the specimen is relatively well preserved with little postmortem distortion. The right zygomatic arch, the right posttympanic and the left paraoccipital processes, as well as the basisphenoid and pterygoid bones are incompletely preserved, while the small premaxillary bones are missing. The dentition of MTLA-5 is complete except for the left P2, which is missing (Pl. 2, fig. 1). Specimen PMMS-107 is a moderately well preserved adult cranium (Pl. 1, figs. 2a, b), missing the premaxillary bones, the rostral third of the palate with the P2 and P3 of both sides, the right supraorbital process, both zygomatic arches, the pterygoid bones, parts of the vomer and the basisphenoid, as well as the right wing of the nuchal crest, the lateral margins of the occiput, and both occipital condyles; the paraoccipital, posttympanic, and postglenoid processes are poorly preserved in both sides. Two adult cranial fragments from locality MTLB may belong to one individual: MTLB-339 is the fragmentarily preserved caudal half of the cranium and MTLB-340 a nearly complete nasal fragment. The cranial morphology of all specimens is very similar. Descriptions are based primarily on the complete cranium MTLA-5, and variation is otherwise noted.

The cranium is large and markedly dolichocephalic. The nasal bones are very thick and broad, and they form a very pronounced, domelike, nasal horn boss with extensive, rough, vascular impressions. In dorsal view, the nasal bones terminate abruptly and their rostral border is very wide and rounded. The internasal suture remains open

	Diceros neumayri			*Dihoplus pikermiensis*			Total: *Diceros* + *Dihoplus*		
	Specimens	MNI	Adult - Juvenile	Specimens	MNI	Adult - Juvenile	Specimens	MNI	Adult - Juvenile
MTLA	57	7	3 - 4	1	1	1 - 0	58	8	4 - 4
MTLB	14	4	2 - 2	0	0	0 - 0	14	4	2 - 2
MTLD	7	2	2 - 0	2	1	1 - 0	9	3	3 - 0
PMMS	29	4	3 - 1	0	0	0 - 0	29	4	3 - 1
MYT	4	1	1 - 0	8	1	1 - 0	12	2	2 - 0
MLN	2	1	1 - 0	0	0	0 - 0	2	1	1 - 0
TOTAL:	113	19	12 - 7	11	3	3 - 0	124	22	15 - 7

Table 1: Comparative distribution of the recovered specimens and minimum number of individuals (MNI) of "*Diceros*" *neumayri* (Osborn, 1900) and *Dihoplus pikermiensis* (Toula, 1906) from Mytilinii Basin, Samos, according to locality and ontogenetic stage.

and deeply marked only along the rostral surface of the nasal horn dome, but it is completely ossified caudally. The ventral surface of the nasal bones is transversally concave and there is no bony nasal septum. In lateral view, the narial incision terminates above the level of the mesial half of P3. The infraorbital foramen is longitudinally level with the deepest point of the narial incision; it is single, large and rounded, and situated above the mesial half of P4. The facial surface of the maxilla is broad and slightly convex. The facial crest is rather weak and fades out above the M1. The root of the zygomatic bone emerges several centimeters above the M2. Underneath, the buccinator region of the maxillary bone is clearly marked along the alveolar processes of the molars. The maxillary tuber is incompletely preserved. The dorsal surface of the frontal bones (cranial roof) is very convex transversally. In-between the level of the supraorbital processes, a smaller, wide and low dome with coarse vascular impressions signifies the presence of a frontal horn boss. The supraorbital process is very strong and projects markedly laterocaudally. A postorbital process is not developed on the frontals. The tips of the lachrymal process are broken off in all specimens, but their base suggests that they must have been moderately developed. Due to the fragmentary surface it is not clear whether the lachrymal foramen was single or double. The rostral border of the orbit terminates above the level of the distal half of M2. The floor of the orbit (dorsal surface of the zygomatic bone) slopes laterally downwards. Only the left zygomatic arch of the cranium MTLA-5 is preserved, but it is distorted and mediodorsally elevated due to postmortem fraction and rotation. Because of this distortion, it inaccurately appears to be upraised and almost reaching the level of the cranial roof in lateral view (Pl. 1, fig. 1). The ventral surface of the articular tubercle for the mandible is gently concave.

The crania MTLA-5 and PMMS-107 retain the frontal and parietal region in relatively good condition with little distortion. In lateral view, the dorsal cranial profile is clearly concave (Pl. 1, figs. 1, 2a). This is manifested in both crania, though somewhat accentuated in MTLA-5 by postmortem distortion, and resembles the condition of certain large-sized specimens of extant *D. bicornis* (e.g. RMNH: Cat-A; MNHN: A.7969). Nonetheless, in the majority of over one hundred crania of *D. bicornis* which we have observed, the depth of the dorsal concavity is generally much more marked. On the other hand, in extant *C. simum*, the dorsal cranial profile is generally much more flattened. Even in this case though, the dorsal concavity of a few specimens of *C. simum* (e.g. SMNS: 49763) appears to overlap with specimens of *D. bicornis*, based on our observations and by the cranial angle measurements conducted by Zeuner (1934) and Loose (1975). In particular, this concerns specimens of the southern subspecies *C. simum simum*, and is a valid subspecific criterion with respect to the northern subspecies *C. simum cottoni* (which has the most flattened condition), as noted by Heller (1913) and statistically evaluated by Groves (1975). In dorsal view, the bilateral oblique parietal crests remain separated and a sagittal crest is not formed (Pl. 1, fig. 2b). Rostrally, the parietal crests smoothly diverge laterally and are parallel to? the temporal lines. Caudally, they curve backwards into the nuchal crests. The nuchal crests are deeply notched in the middle (specimen MTLA-5, Pl. 5, fig. 10). In specimen PMMS-107, the right wing of the occipital crest is missing, but based on the complete left wing, the inference is the same (Pl. 1, fig. 2b). This condition resembles extant *C. simum*, in which the shape of the sagittal notch of the nuchal crests varies from clearly concave to deeply V-shaped. On the contrary, in extant *D. bicornis* the caudal margin of the nuchal crests is nearly straight (not indented) or only slightly concave. In lateral view, the wings of the nuchal crests of both Samos specimens extend caudally beyond the level of the occipital condyles, so that the occipital plane inclines backwards, but not as markedly as in extant *C. simum*. This condition is however more derived with respect to the extant *D. bicornis*, where the nuchal crests do not stretch backwards over the condyles, and the occipital plane remains nearly vertical or even frontward inclined in most specimens (for the polarity of this characteristic also compare the discussion in Antoine, 2002:89; fig. 28).

In caudal view, the occiput has a nearly square outline (Pl. 5, fig. 10). The squamous occipital fossa is deep and demarcated by pronounced bilateral occipital crests. The external occipital protuberance is moderately developed (cranium PMMS-107, surface loss prevents observation on other specimens). The nuchal tubercle is weakly developed. The foramen magnum is ovate, higher than wide. The occipital condyles are reniform. In ventral view, the basilar part of the occipital bone is well preserved in specimen MTLA-5,

Table 2: "*Diceros*" *neumayri* (Osborn, 1900). Measurements of the adult crania (in mm).

Measurements	MTLA-5	PMMS-107
Length from occiput (nuchal crest) to nasal tip	705	680
Length from occiput (nuchal crest) to P2 parastyle	685	—
Length from occipital condyles to nasal tip	710	—
Length from occipital condyles to P2 parastyle	638	—
Length from nasal incision to nasal tip	156	148
Length from rostral border of orbit to nasal tip	310	(305)
Length from rostral border of orbit to nasal incision	172	(168)
Length from occiput (nuchal crest) to lachrymal process	468	—
Length from occiput (nuchal crest) to subraorbital process	425	365
Length from occipital condyle to distal end of M3	282	—
Length from basion to midpoint of mesial level of P2s	592	—
Length from basion to rostral border of choanae	(372)	(348)
Length from rostral bord. choanae to mesial level of P2s	(220)	—
Maximal width of nasals	145	(138)
Width of nasals at nasal incision	140	—
Width at supraorbital processes	(250)	—
Maximal width at zygomatic arches	—	—
Minimal width between parietal crests	53	61
Width at nuchal crests	235	—
Width maximal at paraoccipital processes	(230)	—
Occipital height from ventral border of occipital condyles	220	—
Occipital height from dorsal border of foramen magnum	148	144
Maximal width at occipital condyles	124	—
Width of foramen magnum	36	—
Height of foramen magnum	(50)	—

and reasonably so in specimens PMMS-107 and MTLB-349. In all three specimens, a moderately developed sagittal crest runs along its body, extending from the intercondylar incision to the muscular tubercles. The muscular tubercles are fused into a single large protuberance at the spheno-occipital synchodrosis. The paraoccipital process is long, straight, and slender. The posttympanic process is relatively small and short, and bends forwards. In specimen MTLA-5, the tip of the posttympanic process gently contacts the base of the postglenoid process; in specimen PMMS-107, the two processes remain slightly separated. The postglenoid process is very long, slightly depressed transversally, and its ventral tip gently bends forwards; it is the most prominent of the three processes. None of the specimens preserves the vomer and the pterygoid bones in good condition. In both MTLA-5 and PMMS-107, the rostral margin of the nasopharyngeal passage (choanae) terminates at the protocone level of M3. A nasal spine appears not to be developed, though the caudal surface of the palatine bones is somewhat distorted in both specimens. The palatine processes of the maxilla are rather narrow and fused in the middle. None of the specimens preserves the premaxillary bones.

Juvenile Crania

Two juvenile crania have been recovered during the recent excavations on Samos. MTLA-212 is a fairly complete, uncrushed, juvenile cranium (Pl. 2, figs. 2a, 2b), preserving the entire deciduous dentition in excellent condition (Pl. 4, fig. 6). Due to the incomplete ossification, the specimen is missing the diminutive premaxillary bones, small parts of the nasals' rostral tip, the interparietal, occipital, and basisphenoid bones, as well as the tips of the postglenoid and posttympanic processes. Ontogenetically, the specimen is similar to the juvenile cranium from Kerassia documented by Giaourtsakis et al. (2006) and shows a comparable stage of dental wear and cranial ossification. The principal morphological features are essentially the same as in the adult specimens. Some idiosyncratic features of MTLA-212 that may be noted at this ontogenetic stage are: in lateral view, the nasal incision terminates above the level of the distal half of D2, the infraorbital foramen is placed above the mesial half of D3, and the rostral border of the orbit extends above the distal half of D4; in ventral view, the rostral border of the choanae terminates at the level in-between the D4 and the unerupted M1. The second juvenile cranium, MTLB-43, is very incomplete and severely crushed dorsoventrally; its deciduous dentition is fragmentarily preserved and missing the right D1. The cranial morphology of the new juvenile specimens from Samos does not show any significant difference compared to the juvenile crania of "*Diceros*" *neumayri* from Kerassia, Pikermi, Samos and other Eastern Mediterranean localities that have been recently described and discussed by Giaourtsakis et al. (2006).

Permanent Upper Dentition

Apart from the permanent upper dentition of the two adult skulls, MTLA-5 (Pl. 4, fig. 1) and PMMS-107 (Pl. 4, fig. 3), a set of associated upper teeth, partly attached to broken maxillary fragments, has also been recovered, MTLA-425 (Pl. 4, fig. 2). The three upper dentitions show very similar morphological features, expressed at different ontogenetic stages. Specimen MTLA-425 represents the

		MTLA-5		MTLA-425		PMMS-6	
		right	left	right	left	right	left
P1	L	—	—	—	—	—	—
	Wd	—	—	—	—	—	—
P2	L	36.1	—	—	—	—	—
	Wm	37.0	—	—	—	—	—
	Wd	41.8	—	—	—	—	—
P3	L	44.0	43.6	—	—	—	—
	Wm	53.6	53.8	—	—	—	—
	Wd	50.6	(51.5)	—	—	—	—
P4	L	48.8	49.5	—	48.0	—	50.2
	Wm	62.1	62.4	—	61.8	61.0	61.8
	Wd	54.8	55.7	—	(57.0)	56.3	57.6
M1	L	52.6	52.5	—	—	—	(55.5)
	Wm	62.7	61.6	—	—	62.6	63.4
	Wd	56.3	56.8	—	—	57.2	58.3
M2	L	61.9	61.2	63.0	—	(61.0)	61.8
	Wm	64.7	64.8	67.3	—	(65.5)	66.8
	Wd	55.6	55.9	58.0	—	57.8	58.6
M3	Lb	63.7	64.8	62.1	61.8	66.7	66.9
	Wm	61.2	61.0	58.3	57.6	58.8	59.3
	La	54.0	53.2	52.8	52.3	55.7	55.1
P2-M3		270.0	—	—	—	—	—
P2-P4		121.8	—	—	—	—	—
P3-P4		88.8	88.1	—	—	—	—
M1-M3		158.0	159.0	—	—	161.0	160.0

Table 4: *"Diceros" neumayri* (OSBORN, 1900) from Mytilinii Basin, Samos. Measurements of the upper permanent dentition (in mm).

relatively youngest adult individual, showing the fully erupted M3 at an early stage of occlusal wear. The other two specimens belong to older individuals, with specimen PMMS-107 exhibiting the most advanced stage of occlusal wear of the three. The D1 does not persist in adulthood. The occlusal surface of the teeth is concave, and the enamel is thicker on the sides of the teeth, but thinner around the medisinus. In all teeth, traces of a cement coating can be observed on the buccal wall of the ectoloph and inside the medisinus basin; the strength of the cement coating is similar to that of extant *D. bicornis*, and not as strong and abundant as in *C. simum*. Descriptions are primarily based on the complete dentition of the cranium MTLA-5, and ontogenetic or idiosyncratic variation of other specimens is noted.

The P2 has a nearly square outline and is smaller than the succeeding premolars. As is common in P2s, the metaloph is slightly longer than the protoloph and the mesial width is greater than the distal one. The P2 is also less molariform (sensu HEISSIG, 1989) with respect to p3 and p4, showing an earlier and stronger lingual fusion between protocone and hypocone. At this late stage of wear, no internal secondary folds can be observed. The postfossette is reduced to a small closed fossette in the worn metaloph. The ectoloph is gently convex, bearing only the trace of a very faint paracone fold.

P3 and P4 are similar in morphology; the fourth premolar is somewhat larger than the third one, and has its cross lophs slightly more oblique. Both premolars correspond with the molariform stage of molarization (HEISSIG, 1989). During early and moderate stages of occlusal wear, protocone and metacone remain separated and the entrance of the medisinus is open (e.g. ANTOINE & SARAÇ, 2005: fig. 2A, from Akkaşdaği). Specimen MTLA-5 shows that the protocone and hypocone of P3 become confluent only during the late stage of occlusal wear, whereas in P4 they remain separate longer, even in the old adult PMMS-107, indicating a slightly higher degree of molarization for the last premolar. The mesial and distal cingula are well developed, but they do not project lingually. A reduced, discontinuous, crenellated lingual cingulum is restricted to the base of the entrance of the medisinus. The less worn P3 of MTLA-425 shows the presence of a weak crista and crochet, which have disappeared by wear in specimen MTLA-5. Likewise, the less worn P4s of both specimens show the weak crista and crochet, which are not apparent any more in the much worn P4 of specimen PMMS-107. A medifossette is not formed at any stage of wear. A faint to weak mesial protocone groove is present, but a distal protocone groove and an antecrochet are absent; the distal border of the protocone is markedly convex. The hypocone is slightly smaller than the protocone and lacks both mesial and distal constrictions. The postfossette remains distally open only in the less worn P4 of specimen MTLA-425. On the buccal wall of the ectoloph, the parastyle is not particularly prominent and the parastyle groove is not marked. A paracone fold is present, but weakly developed; it fades gradually out towards the base of the tooth, thus being less apparent in the old adult individual PMMS-107. A metacone fold is absent. A buccal cingulum on the ectoloph is not developed.

The first two molars are morphologically similar. As expected, M1 has a more rectangular outline, whereas M2 is somewhat longer but distally narrower in relation. In both molars, there is no lingual or buccal cingulum. A modest crochet is the only secondary fold that projects into the medisinus valley; a crista is absent. The mesial protocone groove is deeper and better expressed compared to the premolars. A distal protocone groove and an antecrochet are not developed. The parastyle is more marked on M2. The parastyle groove is shallow. A weak to moderate paracone fold is the most prominent vertical fold on the ectoloph, better expressed in the ontogenetically younger specimen MTLA-425. It gradually fades out towards the cervical margin of the tooth, so that it becomes less apparent on the molars of the older adult specimens MTLA-5 and PMMS-107. The mesostyle fold is developed as a broader but less prominent swelling, especially on the M2. A metacone fold is absent, however, the coronal apex of the metacone cusp is sharper and more prominent than the paracone one; their intermediate relief is concave. The distal half of the buccal wall of the ectoloph is gently concave. The metastyle is long, and more pronounced in M2.

The M3 has a subtriangular outline, bearing a continuous ectometaloph. The paracone fold is better marked compared to the previous two molars, as the tooth is less worn. A weak mesostyle swelling is evident in the middle of the ectometaloph. A low and narrow distal cingulum marks the base of the distal side of the hypocone. The mesial cingulum is well developed. The protoloph is rather vertically oriented. The protocone is constricted only by a weak mesial groove; as in the rest of the teeth, a distal protocone groove and an antecrochet are not developed. Likewise, a crochet is present, but no crista. The most notable feature is the presence of a pronounced cingular pillar on the base of the entrance of the medisinus; in specimen PMMS-107, it is even doubled. The occurrence of this cingular pillar, which topographically corresponds to an entostyle, is frequently observed in the last molars of some specimens of *"Diceros" neumayri* (e.g. NHMW: A.4791, from Maragheh; MTA: AK4-212, from Akkaşdaği; SMNK: Ma2.Gips6, from Mahmutgazi).

The morphological properties of the permanent dentition of *"Diceros" neumayri* are more similar to the dentition of extant *D. bicornis*, in particular to the larger and more arid adapted subspecies *D. b. bicornis* and *D. b. chobiensis*. They lack all the advanced specializations of the *Ceratotherium* lineage that has gradually developed a highly hypsodont and plagiolophodont dentition with abrasion-dominated wear. In extant *C. simum*, the teeth are high-crowned and functionally hypsodont (sensu Fortelius, 1982, 1985), with flattened occlusal surface and a flattened mesowear profile (Fortelius & Solounias, 2000); the enamel thickness is rather constant and the cement investment is abundant; the protoloph and metaloph bend markedly distolingually; in the premolars, the protoloph and metaloph fuse after early wear, closing, and the lingual cingulum is virtually absent; a strong crochet and crista are developed, which fuse in the molars and most premolars, during very early stages of occlusal wear, to form a closed medifossette; on the buccal wall of the ectoloph, the paracone fold is completely suppressed by a deep parastyle groove and the mesostyle fold is very prominent; the M3 has a quadrilateral outline with a separate ectoloph and metaloph. These features of the white rhinoceros lineage were gradually established during the Plio-Pleistocene in Africa and reflect its gradual adaptation to an exclusive grass diet (Geraads, 2005; Giaourtsakis et al., in press, Hernesniemi et al., in press). The upper permanent dentition of *"Diceros" neumayri* can be easily distinguished from *Dihoplus pikermiensis* (Geraads, 1988). In *Dihoplus pikermiensis*, the premolars are paramolariform, showing a rapid fusion between protocone and hypocone during early stages of occlusal wear; the paracone fold is stronger, and a metacone fold is present. In the molars of *Dihoplus pikermiensis*, the protocone is constricted by a mesial and a distal groove.

Upper Deciduous Dentition

Deciduous teeth are well-represented in our sample (Table 5). Apart from the dentitions of the two juvenile skulls (MTLA-212, MTLB-43), several sets of associated de-

		MTLA-212		MTLB-43		MTLA -27	MTLA -98	MTLA -521	MTLA -443	MTLA -497	MTLB -87
		right	left	right	left						
D1	L	25.8	26.2	—	22.4				26.3		25.1
	Wd	25.4	25.2	—	21.0				22.2		24.3
D2	L	40.8	41.3	—	36.8	(36.0)	40.7	38.8		—	38.2
	Wm	37.1	36.2	—	35.3	35.2	31.6	32.1		(35.5)	(35.0)
	Wd	37.2	36.4	33.8	34.7	—	(32.0)	33.7		36.4	35.4
D3	L	51.0	50.3	46.8	45.5	45.9	48.3	46.7			44.8
	Wm	45.5	45.8	43.2	42.6	40.8	—	42.3			—
	Wd	43.2	42.8	42.0	41.1	39.1	—	39.6			—
D4	L	59.2	58.8	54.4	53.2						
	Wm	49.1	48.8	49.8	49.4						
	Wd	45.8	46.2	45.8	46.2						
D1-D4		161.0	160.0	—	142.1						
D2-D4		137.4	138.3	—	128.8						
D3-D4		103.8	104.2	96.7	95.0						

Table 6: *"Diceros" neumayri* (Osborn, 1900) from Mytilinii Basin, Samos. Measurements of the upper deciduous dentition (in mm).

ciduous teeth attached to maxillary fragments (MTLA-337, MTLA-27, MTLA-521, MTLB-340), as well as some isolated specimens (MTLA-98, MTLA-443), have been recovered. The deciduous teeth of "*Diceros*" *neumayri* can be easily distinguished from *Dihoplus pikermiensis* (Geraads, 1988; Giaourtsakis et al., 2006). The new specimens from Samos fall within the known variation of the species and confirm the morphological differences compared to *Dihoplus pikermiensis* (compare Giaourtsakis et al., 2006: tab. 3).

Adult Mandibles

PMMS-106 and PMMS-108 are two moderately well preserved mandibles. The first specimen retains a greater portion of the mandibular angle and ascending ramus (Pl. 3, fig. 1), whereas the latter preserves the entire mandibular symphysis intact (Pl. 3, figs. 2a-c); both specimens are missing the mandibular condyles and the coronoid processes. Well-preserved mandible symphyses of "*Diceros*" *neumayri* mandibles are extremely rare (Giaourtsakis et al., 2006), thus specimen PMMS-108 is of particular interest. The stage of dental wear indicates that both mandibles belonged to aged adult individuals. Ontogenetically, specimen PMMS-108 is slightly younger, as the protolophid and the cristid obliqua of the m3 have not become confluent.

The body of the mandible is rather robust. Its ventral border is gently convex. Specimen PMMS-108 preserves the mental foramen, which is oval and placed in front of p2. On the medial surface of the mandibular body, the mylohyoid line forms a longitudinal shallow depression. The mandibular angle is convex, without marked angulation. The elevation of its ventral border is moderate and more similar to extant *D. bicornis*. In extant *C. simum*, the mandibular angle is more obtuse-convex and the elevation of the ventral border stronger. On the lateral side, the masseteric fossa is well defined and demarcated ventrally by a coarse and blunt masseteric ridge. The depression of the masseteric fossa fades out rostrally before the level of m3. On the medial side, the pterygoid fossa is somewhat shallower. Specimen PMMS-106 preserves the mandibular foramen, which is placed below the level of the alveolar arc. The retromolar space is long and curves gently into the rostral border of the ascending ramus.

In dorsal view (Pl. 3, fig. 2b), the mandibular symphysis extends caudally to a point below the distal root of p3. The rostral portion of the symphysis, which extends in front of the premolars, differs from both extant African species. It is absolutely and relatively longer compared to *D. bicornis*, whereas it is absolutely and relatively narrower compared to *C. simum*. Morphologically though, the symphysis of PMMS-108 resembles the symphysis of *D. bicornis* more closely. In lateral view, the elevation of the ventral border of the symphysis is strong but smooth, forming an angle with the horizontal ramus, similar to *D. bicornis*; in *C. simum*, the elevation of the ventral border of the symphysis is much more abrupt. In dorsal view, the dorsal surface of the symphysis is transversally concave throughout its length, as in *D. bicornis*. In *C. simum*, the dorsal surface of the symphysis is concave in-between the premolars, but shallows markedly as the symphysis widens rostrally. Similar to both extant species, the rostral border of the symphysis is convex and slightly notched at its middle point. Two very small and shallow bilateral depressions on the dorsal surface of the rostral border of the symphysis represent remnant di2 alveoli (Pl. 3, fig. 2b). Such remnant alveoli of di2 and/or di1 are frequently present in the symphysis of adult specimens of *D. bicornis* and, occasionally, a rudiment of the milk incisor may persist inside the alveolus (e.g. RMNH: Cat-A; ZMA: 506). Less frequently, such small depressions may also persist in the symphysis of *C. simum*, but they are even more superficial and placed much closer to the middle point of the rostral border of the widened symphysis (e.g. MNHN: 1928-310; ZMA: 6997). In ventral view, the most notable feature of the mandibular symphysis of PMMS-108 is the development of a prominent sagittal crest (Pl. 3, fig. 2c). The presence and strength of this crest is most likely an idiosyncratic feature, since it is occasionally developed in some specimens of extant *D. bicornis* as well (e.g. SMNS: 965; ZMUC: CN.3729).

The mandibular morphology of *Dihoplus pikermiensis* has been recently documented by Giaourtsakis et al. (2006). Well-preserved mandibles of *Dihoplus pikermiensis* can be

Measurements	PMMS-106	PMMS-108
Length of the mandible	—	est. 540
Length until the caudal margin of symphysis	418	est. 410
Maximal length of the symphisis	—	143
Length of the symphisis in front of p2	—	68
Minimal width of symphysis	—	60
Maximal rostral width of symphysis	—	67
Height of mandibular body in front of p3	79	85
Height of mandibular body in front of p4	91	94
Height of mandibular body in front of m1	103	111
Height of mandibular body in front of m2	104	113
Height of mandibular body in front of m3	103	112
Height of mandibular body behind m3	100	108
Width of mandibular body in front of m1	51	58
Width of mandibular body behind m3	58	61

Table 3: "*Diceros*" *neumayri* (Osborn, 1900) from Mytilinii Basin, Samos. Measurements of the adult mandibles (in mm).

distinguished from *"Diceros" neumayri* by the following combination of features: the mandibular angle is more acute; the elevation of the ventral border of the symphysis is smoother; the caudal border of the symphysis terminates mostly well before the level of p3; the portion of the symphysis in front of p2 is longer; the interalveolar margin is somewhat stronger ridged; the symphysis bears permanent second lower incisors rostrally, though small ones, or it features well-formed alveoli if the incisors are not preserved (Gaudry, 1862-67: Pl. 28, fig. 1, 2; Giaourtsakis et al., 2006: figs. 3c, 4).

Juvenile Mandibles

Four mandibular fragments of juvenile individuals (MTLA-179, 242, 371; MTLB-109) are very incompletely preserved. They show a convex ventral border and the presence of the mylohyoid line on the medial side of the mandibular body. Specimen MTLA-179 preserves the mental foramen in front of the mesial root of d2.

Lower Permanent Dentition

The lower permanent teeth in our sample are represented only by the dentitions of the two adult mandibles, PMMS-106 and PMMS-108. Unfortunately, most of the teeth are much worn, concealing details of their occlusal morphology (Pl. 4, figs. 4, 5). Traces of a thin cement coating can be observed on the buccal walls of several teeth.

The d1 does not persist in adulthood. As is common in advanced rhinocerotids, the p2 is small and has a reduced trigonid. In both specimens, the trigonid basin of all premolars is completely worn out. A remnant of the talonid basin shows that it has remained lingually open even at these advanced stages of occlusal wear, excluding the formation of closed fossettids. The p4 is slightly larger than the p3. The lingual aspect of the metaconid and the entoconid is rounded. The buccal wall of the trigonids and talonids is gently convex. There is no mesial vertical groove developed on the buccal wall of the trigonids. The ectoflexid is weakly marked on p2, and moderately marked on p3 and p4. The buccal enamel ridge of the cristid obliqua and the distal enamel ridge of the metalophid nearly form a right angle. There are no lingual or buccal cingula. Traces of a mesial and a distal cingulum can be observed on the mesial and distal sides of the teeth, but generally they do not project on the lingual or buccal sides.

The m1 is the most heavily worn tooth; at this stage of wear, it features a rather shallow ectoflexid. The m2 is slightly wider than m3, but the latter is slightly longer. The paralophid is moderately long and does not reach the level of the lingual wall of the metaconid lingually. In lingual view, the talonid basin is U-shaped. In occlusal view, the lingual enamel, which surrounds the trigonid and talonid basins, is thinner compared to the buccal, distal, and mesial enamel. The hypolophid is rather transversally oriented. The buccal walls of the trigonid and the talonid are gently rounded. The ectoflexid is well-marked and extends down to the cervical margin of the tooth. There are no lingual or buccal cingula developed. Traces of mesial and distal cingula can be observed on the mesial and distal sides of the teeth; occasionally, they may project slightly lingually or buccally. As compared to the extant Dicerotini, the lower dentition of *"Diceros" neumayri* morphologically resembles *D. bicornis* and lacks all derived features of *C. simum*. In *C. simum*, the metaconid and entoconid of the premolars are broader, developing longitudinal buttresses that frequently fuse lingually and close the trigonid and talonid basins forming fossettids. Further, the lingual aspects of the metaconid and entoconid buttresses are flattened or slightly depressed. The labial walls of the trigonid, and sometimes of the talonid, are also flattened or even slightly depressed. The hypolophid of m3, and sometimes of m2, is straighter and nearly longitudinally oriented. Additionally, the enamel thickness in *C. simum* remains rather constant over the entire tooth and the cement coating is abundant.

		PMMS-106		PMMS-108	
		right	left	right	left
p2	L	—	—	30.7	30.9
	Wm	18.0	—	18.7	19.3
	Wd	(21.5)	—	20.6	22.3
p3	L	34.3	35.0	37.8	38.4
	Wm	23.8	23.5	25.4	24.7
	Wd	27.2	27.8	29.3	29.1
p4	L	41.4	41.2	40.8	40.6
	Wm	28.7	28.6	29.6	29.8
	Wd	31.6	30.8	32.8	33.1
m1	L	(43.0)	43.3	45.8	45.1
	Wm	31.5	31.5	29.5	30.2
	Wd	—	33.9	31.2	32.0
m2	L	50.6	49.8	50.5	51.2
	Wm	35.2	35.8	33.4	34.2
	Wd	37.1	37.8	35.7	36.1
m3	Lb	53.4	53.2	52.0	52.7
	Wm	34.3	34.6	34.9	34.2
	Wd	33.4	33.8	33.7	33.2
p2-m3		247.0	—	255.0	257.0
p2-p4		102.0	—	105.6	106.8
p3-p4		76.9	76.2	75.4	77.0
m1-m3		144.2	145.5	150.7	150.8

Table 5: *"Diceros" neumayri* (Osborn, 1900) from Mytilinii Basin, Samos. Measurements of the lower permanent dentition (in mm).

Due to the limited available material and since the lower permanent dentition of the less specialized Rhinocerotinae is quite uniform, it is presently difficult to discuss the constant differences between *"Diceros" neumayri* and *Dihoplus pikermiensis* (Giaourtsakis et al., 2006). Cement traces have not been observed in the teeth of *Dihoplus pikermiensis*. Nevertheless, thin cement coating may be easily destroyed during fossilization, or removed with the matrix during preparation. Teeth of *Dihoplus pikermiensis* seem to be somewhat smaller and have a slightly longer paralophid in the molars. Some proportional differences between the tooth rows may also exist, but more complete mandibles are required to establish unambiguous differences.

		MTLA-179	MTLA-242	MTLA-371	MTLA-239	MTLA-307	MTLB-109
d1	L	21.7					
	Wd	10.4					
d2	L	—			—	33.0	
	Wm	—			—	12.8	
	Wd	—			(16.5)	15.3	
d3	L	43.2	42.4	45.7			
	Wm	16.7	18.9	19.3			
	Wd	18.6	20.7	22.0			
d4	L	—	—	—			—
	Wm	—	—	—			—
	Wd	—	—	—			—

Table 7: "*Diceros*" *neumayri* (OSBORN, 1900) from Mytilinii Basin, Samos. Measurements of the lower deciduous dentition (in mm).

Lower Deciduous Dentition

Only one d1 is present in our sample, attached to the fragmentary juvenile mandible MTLA-179 (Pl. 4, fig. 7). The tooth is double-rooted. It is significantly smaller than the succeeding lower deciduous teeth. The trigonid basin is expressed as an incipient vertical depression on the lingual wall of the protolophid. The talonid basin is V-shaped and fairly deeper than the trigonid basin, but still much reduced compared to the succeeding deciduous molars. The occlusal surface of the tooth is preserved very fragmentarily. The protoconid is the most prominent cusp. In lateral view, the buccal wall of the trigonid is faintly depressed. The buccal aspect of the protoconid is well defined, and the ectoflexid is poorly expressed. The buccal wall of the talonid is broken off. Incipient mesial and distal cingula are present, but no lingual or buccal ones.

Two isolated, unworn d2 have been recovered. Specimen MTLA-307 is complete, whereas specimen MTLA-239 lacks most of the trigonid. The unworn paralophid is double. Its mesial lobe is much smaller and would have been obliterated by additional occlusal wear; its lingual lobe bends slightly distolingually. The unworn protoconid is the highest cusp. The protolophid curves distolingually in occlusal view. The cristid obliqua and the hypolophid are rounded. In buccal view, the ectoflexid is weak to moderate, and fades out towards the cervical margin of the tooth. There is no mesial groove developed on the buccal wall of the trigonid. In lingual view, the trigonid basin is steep, shallow, and widely open. Inside the trigonid basin, a blunt protoconid fold is developed. The talonid basin is deep and markedly V-shaped in lingual view. Towards the base of the crown, the metaconid and entoconid buttresses bend distolingually and mesiolingually respectively, gradually closing the lingual side of the talonid basin. At a moderate stage of occlusal wear, a small fossettid would have been formed by the fusion of the metaconid and entoconid buttresses, as for example in specimen NHMW: 1911-V.44 (Pl. 4, fig. 8). The stage of wear during which the fossettid is formed is rather idiosyncratic, based on comparative observations of 14 specimens in various European collections. Specimen HLMD: SS-77, for example, shows the formation of the fossettid at a very early stage of wear (Pl. 4, fig. 9). Narrow and low mesial and distal cingula are present, but no lingual or buccal ones. The d3 is represented by three specimens, attached to the mandibular fragments MTLA-179, 242, 371. All specimens are at an early stage of wear. The paralophid is bilobed. In specimens MTLA-179 and MTLA-371, the mesial lobe of the paralophid bends distolingually and fuses with the transverse lingual lobe, closing the intermediate paralophid groove and forming a small fossettid (Pl. 4, fig. 7). In specimen MTLA-242, the paralophid groove is mesially open, but it also would have closed after a little additional occlusal wear. The formation of a closed paralophid groove (fossettid) on d3 during the early stages of occlusal wear is the most common condition that we have observed in a comparative sample of 16 individuals of "*Diceros*" *neumayri* (e.g. HLMD: SS-77; Pl. 4, fig. 8). Specimen BMNH: M.4396 from Samos and LGPUT: PNT-14 from the Pentalophos exhibit, for example, show a less common condition, where the two paralophid lobes do not fuse and the paralophid groove remains mesiolingually open (Pl. 4, fig. 10). In all cases, after relatively moderate occlusal wear, the two lobes fuse completely and the paralophid groove, open or closed, disappears, as for example in the specimen NHMW: 1911-V.44 (Pl. 4, fig. 9). The trigonid basin of d3 is lingually open and V-shaped; it is much deeper compared to d2. A blunt protoconid fold is developed inside the trigonid basin. The talonid basin is broader and deeper than the trigonid one. It remains lingually open; a closed fossettid, as in d2, is never formed. The metaconid bends slightly distolingually and its lingual face is rounded. Unworn or little worn entoconids are slightly constricted at their coronal peak by a shallow mesial groove, which fades out rapidly and disappears at moderate stages of wear. On the buccal wall of the trigonid, a mesial vertical groove is mostly absent or visually not apparent. In few individuals, it can occasionally be faintly expressed (e.g. MNHN: SMS-14). The ectoflexid is well marked and terminates cervically before the dental neck. It is oblique, and slightly mesially inclined. The buccal wall of the talonid is slightly convex. The cristid obliqua joins the distally bowed and somewhat oblique hypolophid at a slightly obtuse angle. Narrow mesial and distal cingula are present, but no lingual or buccal ones.

The third deciduous molar of *Dihoplus pikermiensis* can be easily distinguished from "*Diceros*" *neumayri*. The d3 of *Dihoplus pikermiensis* also features a double paralophid, but the mesial lobe is smaller and straight and a closed paralophid groove is never formed. The lingual lobe is longer compared to "*Diceros*" *neumayri*, and its lingual tip frequently bends distolingually. In addition, a shallow but marked and continuous mesial vertical groove is always present on the labial wall of the trigonid of *Dihoplus pikermiensis*. These differences, among others, assert that the type mandible of "*Rhinoceros pachygnathus*, WAGNER 1848" from Pikermi at the collections of BSPG belongs to *Dihoplus pikermiensis*, as commented by HEISSIG (1975a) and GIAOURTSAKIS (2003).

Four d4 are present in our sample, attached to the mandibular fragments MTLA-179, 242, 371 and MTLB-109. All three specimens from MTLA remain unerupted inside the mandibular body and their occlusal surface is partly covered with sediment matrix. The d4 of MTLA-179 is completely preserved (Pl. 4, fig. 7), whereas MTLA-242 and MTL-371 are missing the talonid. The d4 of specimen MTLB-109 retains the buccal profile of the tooth, but the occlusal surface and the lingual portion are very fragmentary preserved. The last deciduous molar is very similar to the permanent ones, lacking the morphological particularities of the three preceding deciduous teeth described above. The paralophid is single and long. The trigonid and talonid basins are deep and lingually broad and open. The protoconid fold inside the trigonid basin is less apparent than in d2 and d3. The labial wall of the trigonid is more rounded and there never is a mesial vertical groove. The ectoflexid is marked, slightly oblique, and terminates cervically before the dental neck. The talonid is somewhat more angular compared to d3, but this can be influenced by the stage of occlusal wear. As in d3, unworn entoconids are slightly constricted at their coronal peak by a shallow mesial groove, which disappears rapidly during moderate stages of wear. Similar to the preceding deciduous molars, narrow and low mesial and distal cingula may be developed, but no lingual or buccal ones.

Postcranial Skeleton

The great majority of the postcranial material in our sample belongs to "*Diceros*" *neumayri*, in particular the specimens from the well-sampled and stratigraphically younger MTL localities of the Adrianos ravine. The occurrence of *Dihoplus pikermiensis* is more balanced in the stratigraphically older locality MYT of the Potamies ravine, but the available material from this site is rather scanty (Table 1). A comprehensive description of the postcranial skeleton of "*Diceros*" *neumayri* is beyond the scope of the present contribution. The most significant morphological differences to the recovered postcranial specimens of *Dihoplus pikermiensis* are documented and discussed in the following section.

Subfamily Rhinocerotinae OWEN, 1845
Tribe Dicerorhinini RINGSTRÖM, 1924

Genus *Dihoplus* BRANDT, 1878

***Dihoplus pikermiensis* (TOULA, 1906)**
(Plates 3, 5)

Localities: Mytilinii-1A, D, (MTLA, MTLD), Adrianos ravine, Mytilinii Basin, Samos, Greece; Mytilinii-3 (MYT), Potamies ravine, Mytilinii Basin, Samos, Greece.
Age: Turolian, late Miocene
Mytilinii-1A, D (MTLA, MTLD): middle Turolian (MN 12), ~7.1 Ma
Mytilinii-3 (MYT): middle Turolian (early MN 12), ~7.3 Ma
Material:
MTLA: Left radius, MTLA-532.
MTLD: Right astragalus, MTLD-8; left astragalus, MTLD-9.
MYT: Right ulna, MYT-123; left scaphoid, MYT-11; right Mc-II, Mc-III, and Mc-IV, MYT-48; left Mc-II, MYT-49; left Mc-III, MYT-67; right Mt-III, MYT-65.

Dihoplus pikermiensis is represented by 11 specimens in our sample; all of them are postcranial elements. The remains belong to at least three individuals, one in each locality (Table 1).

Radius

Specimen MTLA-532 is a complete left radius. The surface of the diaphysis is partially exfoliated, particularly the distal half. It is the only specimen from the well-sampled locality MTLA of Adrianos ravine that can be attributed to *Dihoplus pikermiensis*. The radii of *Dihoplus pikermiensis* can be distinguished by the absolutely and relatively smaller transversal diameters of their proximal and distal epiphysis, and the relatively more slender shaft. The radial tuberosity for the insertion of the biceps tendon is developed as a flattened coarse surface on the medial side of the cranial aspect of the radial column; the lateral tuberosity of the proximal epiphysis (for the lateral collateral ligament) is weakly to moderately developed; the medial margin of the caudal aspect of the distal half of the diaphysis forms a sharp crest; on the cranial surface of the distal epiphysis of the radius, the distolateral tuberosity is not prominent and the furrow for the radial carpal extensor tendon is shallow. On the contrary, the radii of "*Diceros*" *neumayri* have absolutely and relatively larger transversal diameters at the proximal and distal epiphysis, and the shaft is more robust; the radial tuberosity is developed as a more extensive, coarse, shallow depression, and extends to the middle of the radial column, beneath the level of the coronoid process; the lateral tuberosity is stronger and frequently surpasses the lateral border of the radial fovea; the distomedial margin of the caudal aspect of the diaphysis is blunt; on the cranial surface of the distal epiphysis of the radius, the distolateral tuberosity is stronger and particularly prominent in distal view, accentuating the depth of the furrow for the radial carpal extensor tendon.

Ulna

Specimen MYT-123 is a poorly preserved right ulna, missing the olecranon, most of the diaphysis, and the distal epiphysis. The specimen is attributed to *Dihoplus* *pikermiensis* because of the transversal diameter at the coronoid processes, which is absolutely smaller compared to *"Diceros" neumayri.*

Astragalus

Two astragali can be attributed to *Dihoplus pikermiensis*, both originating from the locality MTLD in Adrianos ravine, which comprises the leftovers of an old excavation quarry few meters above the locality MTLA (Kostopoulos et al., this volume). Specimen MTLD-8 is a quite well preserved right astragalus, missing only small segments of the ectal and navicular facets. Specimen MTLD-9 is the incomplete medial half of a left astragalus. Although the astragali of *"Diceros" neumayri* are generally somewhat more robust compared to *Dihoplus pikermiensis*, there is a considerable percentage of overlapping among their measurements, so that osteometric comparisons alone are not sufficient to distinguish the two species. However, the discrimination between the two species can be easily achieved based on numerous, relatively consistent morphological features (Pl. 5, figs. 8, 9). In this section, we will discuss the most reliable and virtually constant ones; additional differential characteristics of a more variable nature do also exist, but their statistical analysis is beyond the scope of the present contribution.

In *Dihoplus pikermiensis*, the sustentacular calcaneal facet is large and has an irregularly subcircular outline; in addition, it always establishes a wide contact (confluent) with the distal calcaneal facet. In *"Diceros" neumayri*, the sustentacular facet has a high-oval outline, and remains separated from the distal calcaneal facet in most specimens, though occasionally a small contact may occur (e.g. AMPG: PA 4600/91, PG 12/88-2 from Pikermi; SMNK: Ma2-Gips.28 from Mahmutgazi). The relationship between the sustentacular and distal calcaneal facets on the astragalus is not always reflected in the corresponding facets of the calcaneus (contra Antoine & Saraç, 2005:617). In fact, as in *"Diceros" neumayri*, in the majority of *Dihoplus pikermiensis* calcanei there is no contact between the sustentacular and distal facets, despite the fact that these facets always have a wide contact on the astragali (e.g. paired specimens of the same individuals: BMNH: M.11321, M.11322, M.11334 from Pikermi).

On the medial side of the bone, the most distinctive feature is the articular surface that corresponds to the medial malleolus of the tibia. In *Dihoplus pikermiensis*, the lower border of this bowed articular stripe is smoothly concave and frequently bears a small convex expansion in its middle, whereas in *"Diceros" neumayri* it generally is more angular and lacks the small expansion. The height of the medial tubercle (Antoine & Saraç, 2005) is not always a constant differing characteristic. Indeed, the majority of *"Diceros" neumayri* specimens have a relatively high-placed medial tubercle, however individuals of *Dihoplus pikermiensis* may occasionally feature a rather high-placed medial tubercle as well (e.g. AMPG: PG 12/88-22, PA 90/4; BMNH: M.11318, M.11334, M.11325.b, M.11325.c from Pikermi). Several differences exist on the lateral side of the bone (Pl. 5, figs. 8, 9). In *Dihoplus pikermiensis*, the bowed articular stripe that articulates with the lateral malleolus of the fibula always retains a rather constant width throughout its length, and always contacts the ectal articular facet for the calcaneus. In *"Diceros" neumayri*, the width of the bowed fibular stripe always narrows smoothly towards its proximal tip, and, occasionally, in some specimens even the contact with the ectal facet is lost. Furthermore, the attachment surface for the lateral talocalcaneal ligament is more extensive and rather flattened in *"Diceros" neumayri*, whereas it is smaller and somewhat more depressed in *Dihoplus pikermiensis*.

Metapodials

Only the locality MYT in Potamies ravine has yielded metapodials of *Dihoplus pikermiensis*. The most prominent specimen is MYT-48, which is comprised of a set of well preserved associated right metacarpals (Pl. 5, fig. 2). The other three isolated metapodials, MYT-49, a left Mc-II, MYT-67, a left Mc-III, and MYT-65, a right Mt-III, are incomplete, preserving more or less only the proximal half of the bone. Metapodials of *Dihoplus pikermiensis* are generally somewhat more slender compared to *"Diceros" neumayri*, but a considerable percentage of overlapping measurements exists, most likely caused by the occurrence of a moderate sexual dimorphism in the two taxa, as well as by temporal and/or spatial intraspecific variation. In particular for the better documented *"Diceros" neumayri*, a gradual size increase from Vallesian to Turolian has been reported (Heissig, 1975a, b, 1996; Kaya, 1994; Giaourtsakis, 2003, in prep.; Fortelius et al., 2003; Antoine & Saraç, 2005).

The two Mc-II of *Dihoplus pikermiensis* in our sample, MYT-48 and MYT-49, may belong to the same individual, as they are metrically and morphologically very similar. The Mc-II is the only metapodial for which reliable differences between *Dihoplus pikermiensis* and *"Diceros" neumayri* have been previously discussed (Geraads, 1988). In *Dihoplus pikermiensis*, an articular facet for the trapezium is always present, as for example in the specimens MYT-48 and MYT-49. In *"Diceros" neumayri* the occurrence of this facet is variable. It can frequently be absent (e.g. AMPG: PG 117/99 from Pikermi; MNHN: GOK-6 from Akkaşdaği; SMNK: Ma1-Nr.98 from Mahmutgazi), and if present, it usually is smaller compared to *Dihoplus pikermiensis* (e.g. AMPG: 12/88 ΠG-354 from Pikermi; BSPG: 1968.VI-359 from Garkin; NHMA: MTLA-388, from Samos). In *Dihoplus pikermiensis*, a longitudinal crest is present on the palmar surface of the shaft, which is never developed in *"Diceros" neumayri*. The strength and continuity of the crest is variable; in most specimens it is clearly marked (e.g. AMPG: PA 4013/91, 12/88 ΠG-307; BMNH: M.11297, M.48190, from Pikermi), but in some specimens it can be quite faintly developed (e.g. AMPG: PA 4008/91, 12/88 ΠG-308; MNHB: MB.Ma.28280, from Pikermi). The complete specimen MYT-48 of *Dihoplus pikermiensis* in our sample features a moderate longitudinal crest. The development of the articular facets for the Mc-III shows some degree of intraspecific variation in both species, but their arrangement is generally different.

In both species, the palmar articular facet, if present (perceptibly), is smaller than the dorsal one. In most specimens of *Dihoplus pikermiensis*, the two facets are mostly either separated (e.g. AMPG: 12/88 ΠG-302, PA 4609/91; BMNH: M.11303.c, from Pikermi) or marked by a deep median notch (e.g. AMPG: 12/88 ΠG 311; BMNH: M.48188, from Pikermi), but occasionally a wider contact may also occur (e.g. MNHB: MB.Ma.28279; BMNH: M.11298, from Pikermi). In *"Diceros" neumayri*, a discrete palmar facet is never developed; it can be either absent (BSPG: 1968.VI 359, from Garkin; MNHN: GOK-6, from Akkaşdaği), or, if present, it is developed as a small continuous expansion of the dorsal facet (e.g. AMPG: 12/88 ΠG-354, from Pikermi; BSPG: 1968.VI 360, from Garkin; SMNK: Ma1-Nr.98, from Mahmutgazi). Both Mc-II specimens of *Dihoplus pikermiensis* in our sample, MYT-48 and MYT-49, clearly show the occurrence of two separated articular facets for the Mc-III.

The most striking difference between the Mc-III of *Dihoplus pikermiensis* and *"Diceros" neumayri* is their outline. In *Dihoplus pikermiensis*, the lateral margin of the shaft is roughly straight, with a relatively faintly expressed curvature towards the proximal end of the bone (Pl. 5, figs. 1, 2b). In *"Diceros" neumayri*, the lateral margin of the shaft is markedly concave in most specimens, in order to accommodate the stronger interosseous rugosity of the Mc-IV, whilst this becomes further accentuated proximally by the somewhat more laterally extended articular facet for the unciform (Pl. 5, figs. 4, 5, 6). On the proximal third of the dorsal surface of the shaft, the rugose attachment surface, which corresponds to the insertion of the carpal extensor muscle, is usually more pronounced in *Dihoplus pikermiensis* than in *"Diceros" neumayri*. In *Dihoplus pikermiensis*, the articular facet for the Mc-II is oblique, whereas it is usually subvertical in *"Diceros" neumayri*. In *Dihoplus pikermiensis*, the sagittal keel of the articular head for the proximal phalanx is generally more pronounced than in *"Diceros" neumayri*, but the difference is not as marked as in the case of Mt-III.

The differences between the Mc-IV of the two taxa are subtle and of a more variable nature. Their separation requires more attention, as it is the combined evaluation of these features that warrants the ascription of isolated bones. In *Dihoplus pikermiensis*, the proximal articular surface for the unciform usually has a subtriangular outline, whereas in *"Diceros" neumayri* it is variably subtriangular-subtrapezoid. On the proximal half of the medial aspect of the shaft, the rugosity for the attachment of the interosseous ligament is usually shorter and stronger in *"Diceros" neumayri* (Pl. 5, fig. 7); in *Dihoplus pikermiensis*, this rugosity is weaker (Pl. 5, fig. 2a) and may frequently bear a shallow longitudinal groove. In *Dihoplus pikermiensis*, the sagittal keel of the articular head for the proximal phalanx is generally sharper and somewhat more pronounced compared to *"Diceros" neumayri*.

Although the overall shape of the Mt-III of both species appears quite similar, there are several reliable differences that allow their distinction. In *Dihoplus pikermiensis*, a small articular facet for the cuboid (between the ectocuneiform and the dorsal Mt-IV facets) is almost always present, whereas this facet is always absent in *"Diceros" neumayri*. In *Dihoplus pikermiensis*, the dorsal border of the articular facet for the ectocuneiform is more frequently and more markedly indented in its middle. Most specimens of *"Diceros" neumayri* lack this indentation, or, if occasionally present, it is only weakly expressed. The only Mt-III of *Dihoplus pikermiensis* in our sample, MYT-65, a proximal half, shows a small articular facet for the cuboid and the marked indentation in the dorsal border of the ectocuneiform facet (Pl. 3, fig. 3). Furthermore, in *Dihoplus pikermiensis*, the bilateral protuberances for the attachment of the collateral ligaments of the fetlock joint appear more pronounced dorsally compared to *"Diceros" neumayri*. In *Dihoplus pikermiensis*, the sagittal keel of the articular head for the proximal phalanx is sharper and more prominent, and (in distal view) it is level with or frequently surpasses the medial rim of the articular head (Pl. 3, fig. 6). In *"Diceros" neumayri* the sagittal keel is markedly less developed and remains below the level of the medial rim of the articular head, as for example in specimen MTLB-21 (Pl. 3, fig. 5). Contrary to Antoine & Saraç (2005: figs. 5d-e), the presence of a fusion between the dorsal and plantar articular facets for the Mt-IV is not characteristic. A direct re-examination of the figured specimen in question from the Turkish locality of Akkaşdaği (MNHN: AKA-45) showed that it actually belongs to *"Diceros" neumayri* and not to *Dihoplus pikermiensis*. The presence of a fusion between the dorsal and plantar articular Mt-IV facets is extremely rare in both species; nearly all specimens that we have examined (N>70) have these two facets separated, though frequently they may come close to one another.

5. Discussion

"Diceros" neumayri was the first recognized fossil relative of the extant African species (Gaudry, 1863) and until the 1960s the only Miocene representative. It is a common element of the Hipparion-faunas of the Subparatethyan (sensu Bernor, 1983, 1984) or Greco-Iranian (sensu Bonis et al., 1992a, b) zoogeographic province and has been firmly documented in numerous localities from Greece (Gaudry, 1863; Weber, 1904; Arambourg & Piveteau, 1929; Geraads, 1988; Geraads & Koufos, 1990; Giaourtsakis, 2003; Giaourtsakis et al., 2006) and Turkey (Heissig, 1975, 1996; Kaya, 1994; Geraads, 1994; Fortelius et al., 2003; Antoine & Saraç, 2005), as well as from the locality of Maragheh in Iran (Osborn, 1900; Thenius, 1955) and Eldari-2 in Caucasus (Tsiskarishvili, 1987). The reported occurrence of the species in the Vienna Basin (Thenius, 1956) was revised as a *Brachypotherium* (Giaourtsakis et al., 2006). Some specimens from Spain reported as *Diceros pachygnathus* by Guérin (1980) were correctly assigned to *Dihoplus schleiermacheri* by Cerdeño (1989). Specimens referred to as *Rhinoceros pachygnathus* from Mont Léberon, France (Gaudry, 1873) and Baltavar, Hungary (Pethő,

1884), also belong to *Dihoplus schleiermacheri* (pers. obs. at MNHN and MAFI). A much worn P2 from Sahabi, Libya, reported as *Diceros neumayri* by BERNOR et al. (1987: fig. 15), is best referred to as Rhinocerotidae indet., since it is much worn and does not bear any diagnostic features. The systematic relationships among the known members of the tribe Dicerotini have been recently revised by GIAOURTSAKIS et al. (in press). The Late Miocene *"Diceros" neumayri* forms a separate, monophyletic, extra-African evolutionary lineage with no Pliocene descendants. The dispersal of this lineage in the Eastern Mediterranean and adjacent regions was followed by the gradual establishment of a unique combination of primitive and derived craniodental features, as well as some autapomorphies, notably in the postcranial skeleton (GIAOURTSAKIS et al., in press). Based on the available fossil record, the split between the two extant Dicerotini lineages took place in Africa during the Miocene. The highly derived anatomical specializations of the *Ceratotherium* lineage towards an exclusive grazing diet were gradually established during the course of the Plio-Pleistocene, following the rapid expansion of open grasslands in Africa (GIAOURTSAKIS et al., in press; HERNESNIEMI et al., in press). Presently, both extant species, *D. bicornis* and *C. simum*, are considered critically endangered, due to relentless hunting and poaching for their horn and hide, as well as destruction or of their habitats, which have caused a dramatic decline of their population numbers during the last century (EMSLIE & BROOKS, 1999).

The known record of *Dihoplus pikermiensis* in the Southeastern Mediterranean is relatively more restricted compared to *"Diceros" neumayri*. The taxon is best known from the locality of Pikermi, but its presence has also been documented in several other Greek localities such as Halmyropotamos, Kerassia and Samos (GAUDRY, 1863; WEBER, 1904; MELENTIS, 1967, 1969; GERAADS, 1988; GIAOURTSAKIS, 2003; GIAOURTSAKIS et al. 2006), as well as in Veles, FYR of Macedonia (SCHLOSSER, 1921), and some Turkish localities (HEISSIG, 1975a, 1996; GERAADS, 1994; FORTELIUS et al., 2003; ANTOINE & SARAÇ, 2005). Unfortunately, the available data about the Late Miocene rhinocerotid assemblages in other Balkan countries is presently insufficient. *Dihoplus pikermiensis* is morphologically similar to its Vallesian forerunner, *Dihoplus schleiermacheri* (KAUP, 1832), which is best known from Central and Western European localities (GUÉRIN, 1980; CERDEÑO, 1989; HEISSIG, 1996). The type specimen of the latter species comes from the Vallesian locality of Eppelsheim in Germany and is comprised of a nearly complete but somewhat exfoliated cranium, HLMD: DIN-1932 (KAUP, 1834: tab. X, fig. 1; GIAOURTSAKIS & HEISSIG, 2004: fig. 1.4); a second, less complete skull, some mandibles, as well as a good amount of supplementary dental and postcranial specimens are also known from the type and nearby localities. The differences between the Vallesian skulls and mandibles from Eppelsheim and the Turolian ones from Pikermi justify the ascription of the two populations to different species. *Dihoplus schleiermacheri* retains several plesiomorphic features, such as the presence of both upper and lower functional incisors, the presence of a sagittal crest, and the less retracted orbit (GERAADS, 1988; GIAOURTSAKIS et. al., 2006). The presence of *Dihoplus* in Western and Central Europe continues uninterrupted during the Turolium; its specimens are commonly also referred to *Dihoplus schleiermacheri* (GUÉRIN, 1980; CERDEÑO, 1989, 1997; HEISSIG, 1996), but complete crania are missing to affirm the exact relationships of these populations with respect to the Eastern Mediterranean *Dihoplus pikermiensis*. Another species of this lineage is *Dihoplus ringstroemi* (ARAMBURG, 1959), which is mainly known from several Chinese and some Russian Turolian localities. This species is quite larger and cranially slightly more derived compared to *Dihoplus pikermiensis*, apparently adapted to cope with somewhat more open habitats (RINGSTRÖM, 1924; DENG, 2006). The terminal species of the genus in Europe, *Dihoplus megarhinus* (DE CHRISTOL, 1835), is a potential descendant of *Dihoplus schleiermacheri - pikermiensis* that survived successfully into the Pliocene (GUÉRIN, 1980; HEISSIG, 1996). During the course of the Pliocene, *Dihoplus* was gradually replaced by the highly derived dicerorhine lineages of *Stephanorhinus* and *Coelodonta* that roamed and dominated Eurasia during the Plio-Pleistocene (GUÉRIN, 1980, 1989; HEISSIG, 1989; FORTELIUS et al., 1993; TONG, 2000; DENG, 2002). The terminal woolly rhino, *Coelodonta antiquitatis*, even survived long enough to be depicted in cave paintings by the Palaeolithic man (RUSPOLI, 1987; CLOTTES, 2003). It is remarkable that all three aforementioned genera (*Dihoplus*, *Stephanorhinus*, *Coelodonta*) are morphologically more derived compared to their closest extant relative, *Dicerorhinus sumatrensis*, justifying the frequent designation of the latter as a living fossil among the rhinoceroses. An embarrassing irony; the Sumatra rhino managed to successfully survive millions of years protected in the montane cloud forests and lowland subtropical rainforests of the Indomalaya ecozone, but nowadays faces the threat of extinction as a result of the harsh poaching and destruction of its habitats by human activities.

6. Paleoecological and Biogeographical Remarks

As discussed above, the dentition of *"Diceros" neumayri* is morphologically and functionally more similar to the dentition of the extant browsing *Diceros bicornis*, and is missing nearly all derived features of the highly specialized dentition of the extant grazing *Ceratotherium simum* (HEISSIG, 1975b; GERAADS, 1988; GIAOURTSAKIS et al., in press). In particular, it very closely resembles the dentition of the larger and more arid-adapted extant subspecies *D. b. bicornis* and *D. b. chobiensis*. However, the cranial morphology and the robust postcranial proportions of *"Diceros" neumayri* are more derived compared to any extant subspecies of *D. bicornis*. The available Eastern Mediterranean record of *"Diceros" neumayri* shows a series of gradual adaptations of this lineage throughout the Vallesian and Turolian, to cope with increasingly open and/or seasonal environments and their nutritionally inferior forage. These include, for instance, the gradual size growth, the lengthening and lowering of the skull, the strengthening of the mesostyle swelling and flattening of the ectoloph profile in the molars, and the gradual increase of the robustness of the appendicular skeleton (Heissig, 1975a, b; Giaourtsakis et al., 2006, in press). These adaptations supported its ability to dwell in more open and dry habitats and utilize more abrasive forage such as bushy vegetation or even soft grasses, when other resources became occasionally or seasonally unavailable.

These gradual anatomical adaptations and the shift towards a coarser, mixed diet in the lineage of the extra-African late Miocene *"Diceros" neumayri* are not surprising. The extant *Diceros bicornis* exhibits a noteworthy degree of flexibility, shifting its food preferences seasonally according to circumstances and availability (Hall-Martin et al., 1982; Oloo et al., 1994). It is even able to utilize plants that have heavy morphological and chemical defenses against most other herbivores (Loutit et al., 1987). Extant black rhinoceroses are able to feed on a wide variety of plant species. Goddard (1968) reported 191 species of plants in Ngorongoro (Tanzania) browsed by black rhinoceroses, while Leader-Williams (1985) reported 220 species in Luangwa Valley (Zambia) and Hall-Martin et al. (1982) recorded 111 species in Addo (South Africa). Even in the extremely arid Darmaland in Northern Namibia, the desert black rhinoceros utilized 74 out of the 103 plant species encountered (Loutit et al., 1987). Small quantities of grass can be consumed together with succulent plants during the dry periods. However, in very dry seasons, excessive consumption of forage with low nutritional value may lead to substantial death rates due to malnutrition (Dunham, 1985, 1994).

Contrary to *"Diceros" neumayri*, the less specialized craniodental and postcranial adaptations of *Dihoplus pikermiensis* suggest that it was a devoted and more selective browser, with a preference for more closed and temperate habitats (Guérin, 1980; Heissig, 1996; Fortelius et al., 2003; Giaourtsakis et al., 2006). Nevertheless, *Dihoplus pikermiensis* was most likely capable to browse a greater amount and variety of plants than its closest living match, the Sumatran rhino *Dicerorhinus sumatrensis*, as indicated by its significantly larger size and the relatively higher crowned, but still functionally brachydont dentition (sensu Fortelius, 1982, 1985). In this context, *Dihoplus pikermiensis* might probably have exploited niches comparable to riverine woodland or open forests, more akin to certain forest-adapted subspecies of the extant browsing *Diceros bicornis*, rather than the humid tropical montane forests inhabited by its significantly smaller-sized and more plesiomorphic extant relative *Dicerorhinus sumatrensis*.

Based on their differentiated paleoecological adaptations, Giaourtsakis et al. (2006) proposed a niche and resource partitioning with limited competition between *"Diceros" neumayri* and *Dihoplus pikermiensis*, and suggested that their relative occurrence in well-sampled Late Miocene localities may offer valuable paleoenvironmental implications. The available rhinoceros material from the stratigraphically older horizons of Samos is too scant to allow any reliable interpretation, as only two specimens of *"Diceros" neumayri* from MLN have been recorded. The material from the intermediate level MYT is also limited, comprising just 12 specimens: 8 specimens representing at least 1 individual belong to *Dihoplus pikermiensis* and 4 specimens representing at least 1 individual belong to *"Diceros" neumayri*. Though it might be expected that this figure could change in favor of *"Diceros" neumayri*, when more material from this locality becomes available, the accentuated occurrence of *Dihoplus pikermiensis* at MYT could be a preliminary indication of somewhat more closed habitats with respect to the stratigraphically younger MTL faunal assemblage. This feeble signal is also in agreement with the paleoecological implications from the equids, bovids and giraffids of the locality (Koufos et al., this volume-b).

From the stratigraphic younger MTL faunal assemblage (MTLA, MTLB, MTLD, PMMS), a reliable sample of 110 specimens has been recovered, representing a minimum number of 19 individuals (Table 1). 97% of the specimens and 90% of the minimum number of individuals belong to *"Diceros" neumayri*, signifying thus a significant interspecific dominance over *Dihoplus pikermiensis*. These figures are in marked contrast to Pikermi (Giaourtsakis et al., 2006; Giaourtsakis, in prep.), where at least 70% of the specimens (sample size >1100) belong to *Dihoplus pikermiensis*, and suggest the expansion of more open and dry habitats on Samos, at least during the time interval of the MTL stratigraphic level. Furthermore, *"Diceros" neumayri* from MTL appears to be slightly more advanced dentally and postcranially compared to Pikermi. Its somewhat larger and more robust appendicular skeleton implies the necessity to cope with more open landscapes, whereas the flattening of the ectoloph by reduction of the paracone fold and strengthening of the mesostyle bulge may suggest an increase of the abrasive component in its diet (Heissig, 1975a; 1996). The evolutionary stage of *"Diceros" neumayri* from the Samos MTL faunal assemblage corresponds well with synchronic localities from Anatolia, such as Garkin and Mahmutgazi. Turkish Turolian localities have predominately yielded *"Diceros" neumayri*, whereas *Dihoplus pikermiensis* remains a very rare element (Heissig, 1975, 1996; Fortelius et al., 2003; personal observations at BSPG, SMNK, MNHN). The well-sampled locality of Akkaşdaği (Antoine & Saraç, 2005) demonstrates a similar marked interspecific dominance of *"Diceros" neumayri* versus *Dihoplus pikermiensis*, as in the Samos MTL assemblage. In addition, *"Diceros" neumayri* from Akkaşdaği is metrically quite larger compared to the MTL population of Samos, which could either indicate a slightly younger age for Akkaşdaği and/or expansion of more open habitats in that locality. In addition, *"Diceros" neumayri* is the only Rhinocerotinae present in the well-sampled localities of the Maragheh sequence in Iran (Thenius, 1955; Geraads, 1988; personal observations at MNHN and NHMW).

Apart from the two horned rhinocerotid taxa discussed, the presence of the hornless genus *Chilotherium* in the fauna of Samos, which is known from previous excavations, is also notable (WEBER, 1905; ANDREÉ, 1921; DREVERMANN, 1930; LEONARDI, 1947; HEISSIG, 1975b; LEHMANN, 1984). Specimens of *Chilotherium* can be found in all major fossil collections from Samos. (NHMW, SMNS, HLMD, GPMM, SMF, GPMH, AMPG, MGPP, AMNH, BMNH). The marked prevalence of cranial material in some collections (GPMH, SMF, MGPP, SMNS, HLMD) most likely represents a biased selective purchase from fossil dealers. The available material from all collections indicates that *Chilotherium* was fairly more common than *Dihoplus* on Samos, but it has also remained significantly less frequent compared to the dominant "*Diceros*" *neumayri*. This figure is in accordance with the extensive record from Anatolia, where *Chilotherium* emerges as the second most frequent rhinocerotid during the course of the Late Miocene, showing gradual specializations towards an increasingly abrasive diet (HEISSIG, 1975a, 1975b, 1996; FORTELIUS et al., 2003). The lack of *Chilotherium* during the recent excavations on Samos may be related to the limited material, particularly from the stratigraphically older localities of Mytilinii-3 (MYT) and Mytilinii-4 (MLN) of the Potamies ravine. Its absence so far from the stratigraphically younger and better sampled localities of Mytilinii-1 (MTL, PMMS) of the Adrianos ravine is more conspicuous, but also requires further sampling for definite conclusions. It can be presently considered as significant only with respect to the dominant "*Diceros*" *neumayri*. However, it may not be regarded as decisive compared to *Dihoplus pikermiensis*, since the latter is also scarce in Mytilinii-1 and represented only by three specimens out of 107 (Table 1). In the well-sampled and somewhat synchronic Turkish locality of Akkaşdaği, the occurrence of *Chilotherium* and *Dihoplus* is correspondingly very limited compared to the dominant "*Diceros*" *neumayri*, the latter comprising more than 90% of the total number of specimens (ANTOINE & SARAÇ, 2005).

Another less specialized hornless taxon present in the Eastern Mediterranean during the Late Miocene is *Acerorhinus*. *Acerorhinus* is markedly absent from Samos, apparently on stratigraphical and ecological grounds. In stratigraphically controlled localities of Anatolia, the presence of *Acerorhinus* is primarily documented during the Vallesium (HEISSIG, 1975a, 1975b, 1996; FORTELIUS et al., 2003). The Vallesian specimens from Anatolia are very similar to the type species *Acerorhinus zernowi* (BORISSIAK 1914, 1915), described from the MN 9 locality of Sebastopol in the Crimea. Their dental mesowear pattern suggests that it was a browser or a browser with a limited mixed-feeding capability (FORTELIUS et al., 2003). At the beginning of the Turolian, the presence of plesiomorphic *Acerorhinus* seems to fade out in Anatolia. In the upper fossiliferous level of Upper Kavakdere in Sinap (ca. 8,1 Ma), the taxon is replaced by a more specialized form (*Acerorhinus* n.sp. of FORTELIUS et al., 2003), which actually shows stronger affinities with the derived genus *Shansirhinus* recently revised by DENG (2005). In continental Greece, plesiomorphic *Acerorhinus* is present in the Vallesian locality of Pentalophos, where it coexists with *Chilotherium* (GERAADS & KOUFOS, 1990, FORTELIUS et al., 2003). Notably, plesiomorphic *Acerorhinus* persists in the temperate habitats of the Turolian locality of Pikermi, where *Chilotherium* is markedly absent (GIAOURTSAKIS, 2003). On the contrary, derived *Chilotherium* is the dominant rhinocerotid in the well-sampled localities of Maragheh in Iran, where *Acerorhinus* remains a very rare element. From the locality of Maragheh we must also add the occurrence of the massive elasmothere *Iranotherium morgani* (MEQUENEM, 1924; ANTOINE, 2002), with a highly specialized hypsodont dentition, as the only effective grazer among the taxa discussed.

The marked differences in the relative distribution and abundance of rhinocerotid taxa among the Turolian localities of the Eastern Mediterranean and adjacent regions appear to be related with environmentally-controlled provincial differences. Localities in the western margin of the Greco-Iranian/Subparatethyan zoogeographic province provided more areas with denser tree coverage and more temperate conditions favored by *Dihoplus pikermiensis*, which dominates over "*Diceros*" *neumayri*; in addition, specialized *Chilotherium* is a very rare element and plesiomorphic *Acerorhinus* persists. In the central and eastern parts of the Greco-Iranian/Subparatethyan zoogeographic province (Samos, Turkish localities, Maragheh) the presence of *Dihoplus pikermiensis* gradually decreases and "*Diceros*" *neumayri* emerges as the dominant horned rhinoceros; furthermore, the occurrence of derived *Chilotherium* becomes progressively more frequent, and it even turns up dominant at Maragheh, where we also encounter the massive elasmothere *Iranotherium morgani*. These gradual changes are markedly associated with the more rapid expansion of open and arid habitats in the central and eastern parts of the Greco-Iranian/Subparatethyan zoogeographic province during this period of time. Analogous strong evidence is provided by the relative distribution of other herbivores in the region, including equids, chalicotheres, bovids and giraffids, as well as by the paleoecological analysis of the faunal assemblages as a whole (KOUFOS et al., this volume-b).

7. Acknowledgements

The excavations on Samos have been supported by the Prefecture of Samos and the "Konstantinos and Maria Zimalis" Foundation. The Municipality of Mytilinii provided generous assistance, too. The Natural History Museum of the Aegean offered us the premises for the preparation and storage of the fossils. I would like to sincerely thank Prof. G. Koufos for inviting me to study the rhinoceros material of the recent paleontological expeditions on Samos. I am also grateful to D. Kostopoulos and D. Vlachou for their kind assistance before and during my visit to the collections of the Natural History Museum of the Aegean. For providing access to specimens under their care, I am indebted to M. Dermitzakis, G. Theodorou, S. Roussiakis (AMPG); J. Hooker, A. Currant, R. Sabin (BMNH); K. Heissig (BSPG); G. Rabeder, D. Nagel (IPUW); G. Koufos, D. Kostopoulos (LGPUT); P. Tassy, C.

Sagne, C. Lefevre, J. Cuisin, L. Viva, J.-G. Michard (MNHN); O. Hampe, N. Klein (NHMB); G. Höck, F. Spitzenberger, B. Herzig (NHMW); F. Schrenk, G. Plodowski (SMF); E. Frey, H.W. Mittmann (SMNK); E. Heizmann (SMNS); L. van de Hoek Ostende, H.J. van Grouw (RMNH); A. Rol (ZMA); H. Baagøe, M. Andersen (ZMUC). I would like to thank D. Geraads for reviewing the manuscript and providing useful comments. Financial support for comparative studies was provided by the Deutscher Akademischer Austausch Dienst (DAAD), the European Commission's Research Infrastructure Action (EU-SYNTHESYS: GB-TAF-574, FR-TAF-1226, NL-TAF-2513, FR-TAF-2545, DK-TAF-3765), and the Research for Human Origin Initiative (RHOI, under NSF award BCS-0321893).

8. References

Andree, J., 1920. Rhinocerotiden aus dem Unterpliozän von Samos. — Paläontologische Zeitschrift, **20**:189–212, Berlin.

Antoine, P.O., 2002. Phylogénie et évolution des Elasmotheriina (Mammalia, Rhinocerotidae). — Mémoires du Muséum national d'Histoire naturelle, **188**:1–359, Paris.

Antoine, P.O. & Saraç, G., 2005. Rhinocerotidae (Mammalia, Perissodactyla) from the late Miocene of Akkaşdaği, Turkey. — [in:] S. Sen (ed.), Geology, mammals and environments at Akkaşdaği, late Miocene of Central Anatolia. — Geodiversitas, **27** (4):601–632, Paris.

Arambourg, C., 1959. Vertébrés continentaux du Miocène supérieur de l'Afrique du Nord. — Publications du service de la carte géologique de l'Algérie (nouvelle série). Paléontologie, Mémoire, **4**:1–159, Algiers.

Arambourg, C. & Piveteau, J., 1929. Les Vertébrés du Pontien de Salonique. — Annales de Paléontologie, **18**:1–82, Paris.

Baron, R., 1999. Anatomie comparée des mammifères domestiques. Tome 1 Ostéologie, 4ème édition. — pp. 761, Paris (Vigot éditions).

Bernor, R.L., 1983. Geochronology and zoogeographic relationships of Miocene Hominoidea. — [in:] Ciochon , R.L. & Corruccini, R.S. (eds.). New Interpretations of Ape and Human Ancestry. — 21–64, New York (Plenum Press).

Bernor, R.L., 1984. A zoogeographic theater and biochronologic play: The time/biofacies phenomena of Eurasian and African Miocene mammal provinces. — Paléobiologie Continentale, **14**:121–142, Montpellier.

Bernor, R.L., Heissig, K. & Tobien, H., 1987. Early Pliocene Perissodactyla from Sahabi, Libya. — [in:] Boaz, N., El Arnauti, A., Gaziry, A., Heinzelin, J. de, & Boaz, D.D. (eds.). Neogene Paleontology and Geology of Sahabi. — 233–254, New York (Alan Liss).

Borissiak, A., 1914. Mammifères fossiles de Sebastopol, I. — Trudy Geolegicheskago Komiteta. Novaja Seria, **87**:1–154, St. Petersburg.

Borissiak, A., 1915. Mammifères fossiles de Sebastopol, II. — Trudy Geolegicheskago Komiteta. Novaja Seria, **137**:1–45, St. Petersburg.

Brandt, J., 1878. Tentamen synopseos rhinocerotidum viventium et fossilium. — Mémoires l'Académie Impériale des Sciences de St. Pétersbourg 7ème Série **26**(5):1–66, St. Petersburg.

Cerdeño, E., 1989. Revisión de la sistemática de los rinocerontes del Neógeno de España. — Colección Tesis Doctorales Universidad Complutense de Madrid, 306/89:1–429, Madrid.

Cerdeño, E., 1995. Cladistic analysis of the Family Rhinocerotidae. — American Museum Novitates, **3143**:1–25, New York.

Cerdeño, E., 1997. Rhinocerotidae from the Turolian site of Dorn-Dürkheim 1 (Germany). — Courier Forschungsinstitut Senckenberg, **197**:187–203, Frankfurt.

Christol, J. de, 1834. Recherches sur les caracteres des grandes especes de rhinoceros fossiles. 4 [quarto], 72 pp, Montpellier.

Clottes, J., 2003. Return To Chauvet Cave, Excavating the Birthplace of Art: The First Full Report. — pp. 232, London (Thames & Hudson).

Deng, T., 2002. The earliest known woolly rhino discovered in the Linxia Basin, Gansu Province, China. — Geological Bulletin of China, **21**(10):604–608, Beijing.

Deng, T., 2005. New cranial material of *Shansirhinus* (Rhinocerotidae, Perissodactyla) from the Lower Pliocene of the Linxia Basin in Gansu, China. — Geobios, **38**:301–313, Lyon.

Deng, T., 2006. Neogene Rhinoceroses of the Linxia Basin (Gansu, China). — Courier Forschungsinstitut Senckenberg, **256**:43–56, Frankfurt a. M.

Drevermann, F., 1930. Aus der Zeit des dreizehigen Pferdes. — Natur und Museum, **60**(1):2–13, Frankfurt a. M.

Dunham, K.M., 1985. Ages of black rhinos killed by drought and poaching in Zimbabwe. — Pachyderm, **5**:12–13, Nairobi.

Dunham, K.M., 1994. The effect of drought on the large mammal populations of the Zambezi riverine woodlands. — Journal of Zoology, **234**:489–526, London.

Emslie, R. & Brooks, M., 1999. African Rhino. Status survey and conservation action plan. — IUCN/SSC African Rhino Specialist Group, pp. 92, IUCN, Gland–Switzerland–Cambridge.

Forsyth-Major, C.I., 1888. Sur un gisement d'ossements fossiles dans l'île de Samos contemporains de l'âge de Pikermi. — Comptes Rendus Hebdomadaires des Séances de l'Académie des Sciences, **107**:1178–1181, Paris.

Forsyth-Major, C.I., 1891. Considérations nouvelles sur la faune de vertébrés du Miocène supérieur dans l'île de Samos. — Comptes Rendus Sommaires Société Géologique de France, **113**:608–610, Paris.

Forsyth-Major, C.I., 1894. Le gisement ossifère de Mytilinii et catalogue d'ossemens fossiles. — Bridel C. & Cie (eds.), Lausanne.

Fortelius, M., 1982. Ecological aspects of dental functional morphology in the Plio-Pleistocene rhinoceroses of Europe. — [in:] Kurtén, B. (ed.). Teeth: form, function and evolution. — 163–181, New York (Columbia University Press).

Fortelius, M., 1985. Ungulate cheek teeth: developmental, functional, and evolutionary interrelations. — Acta Zoologica Fennica, **180**:1–76, Helsinki.

Fortelius, M., Heissig, K., Saraç, G., & Sen, S. 2003. Rhinocerotidae (Perissodactyla). — [in:] Fortelius, M., Kappelman, J., Sen, S. & Bernor, R.L. (eds.), Geology and paleontology of the Miocene Sinap Formation, Turkey. — 282–307, New York (Columbia University Press).

Fortelius, M., Mazza, P. & Sala, B., 1993. *Stephanorhinus* (Mammalia, Rhinocerotidae) of the Western European Pleistocene, with a revision of Stephanorhinus etruscus (Falconer, 1868). — Palaeontographia Italica, **80**:63–155, Pisa.

Gaudry, A., 1862–67. Animaux fossiles et géologie de l'Attique. [The chapter on the rhinoceroses was published in 1863]. — pp. 472, Paris (F. Savy editions).

Gaudry, A., 1873. Animaux fossiles du Mont Léberon (Vaucluse): étude sur les vertébrés. — pp.180, Paris (F. Savy éditions).

Geraads, D., 1988. Révision des Rhinocerotidae (Mammalia) du Turolien de Pikermi. Comparaison avec les formes voisines. — Annales de Paléontologie, **74**:13–41, Paris.

Geraads, D., 1994. Les gisements de Mammifères du Miocène supérieur de Kemiklitepe, Turquie: 4. Rhinocerotidae. — Bulletin du Muséum National d'Histoire Naturelle, 4ème sér., C, **16**:81–95, Paris.

Geraads, D., 2005. Pliocene Rhinocerotidae (Mammalia) from Hadar and Dikika (Lower Awash, Ethiopia), and a revision of the origin of modern African rhinos. — Journal of Vertebrate Paleontology, **25**(2):451–461, Northbrook.

Geraads, D. & Koufos, G.D., 1990. Upper Miocene Rhinocerotidae (Mammalia) from Pentalophos-1, Macedonia, Greece. — Palaeontographica, **210**:151–168, Stuttgart.

Getty, R., 1975. Sisson and Grossman's: The anatomy of the domestic animals, Volume 1. — pp. 1211, Philadelphia, Pennsylvania (W.B. Saunders).

Giaourtsakis, I.X., 2003. Late Neogene Rhinocerotidae of Greece: distribution, diversity and stratigraphical range. — [in:] Reumer, J.W.F. & Wessels, W. (eds.). Distribution and migration of Tertiary mammals in Eurasia. — Deinsea, **10**:235–253, Rotterdam.

Giaourtsakis, I.X. & Heissig, K., 2004. On the nomenclatural status of *Aceratherium incisivum* (Rhinocerotidae, Mammalia). — [in:] Chatzipetros, A.A. & Pavlides, S.B (eds.). Proceedings of the 5th International Symposium on Eastern Mediterranean Geology, **1**:314–317, Thessaloniki.

Giaourtsakis I.X., Theodorou, G., Roussiakis, S., Athanassiou, A., & Iliopoulos, G., 2006. Late Miocene horned rhinoceroses (Rhinocerotinae, Mammalia) from Kerassia (Euboea, Greece). — Neues Jahrbuch für Geologie und Paläontologie, Abhandlungen, **239**:367–398, Stuttgart.

Giaourtsakis, I.X., Pahlevan, C., & Haile-Selassie, Y., (in press). Chapter 14: Rhinocerotidae. — [in:] Haile-Selassie, Y. & Wolde, G. (eds), *Ardipithecus kadabba*: Late Miocene evidence from Middle Awash, Ethiopia. — 429–468, Berkeley (University of California Press).

Groves, C.P. 1975. Taxonomic notes on the white rhinoceros *Ceratotherium simum* (Burchell, 1817). — Säugetierkundliche Mitteilungen, **23**(3):200–212, München.

Groves, C.P., 1983. Phylogeny of the living species of rhinoceros. — Zeitschrift für Zoologische Systematik und Evolutionsforschung, **21**:293–313, Hamburg.

Guérin, C., 1980. Les Rhinocéros (Mammalia, Perissodactyla) du Miocène terminal au Pléistocène supérieur en Europe occidentale. Comparaison avec les espèces actuelles. — Documents des Laboratoires de Géologie de la Faculté des Sciences de Lyon, **79**:1–1185, Lyon.

Guérin, C., 1989. La famille des Rhinocerotidae (Mammalia, Perissodactyla): systématique, histoire, évolution, paléoécologie. — Cranium, **6**(2):3–14, Utrecht.

Goddard, J., 1968. Food preferences of two black rhinoceros populations. — East African Wildlife Journal, **6**:1–18, Oxford.

Hall-Martin, A.J., Erasmus, T. & Botha, B.P., 1982. Seasonal variation of diet and faeces composition of Black Rhinoceros (Diceros bicornis) in the Addo Elephant National Park. — Koedoe, **25**:63–82, Tygervalley.

Heller, E., 1913. The white rhinoceros. — Smithsonian Miscellaneous Collection, **61**(1):1–56, Washington.

Heissig, K., 1975a. Rhinocerotidae aus dem Jungtertiär Anatoliens. — Geologisches Jahrbuch (B), **15**:145–151, Hannover.

Heissig, K., 1975b. Rhinocerotidae aus den Hipparion-Faunen Anatoliens. — Unpublished Habilitation Thesis, pp. 538, Department of Geosciences, University of Munich.

Heissig, K., 1981. Probleme bei der cladistischen Analyse einer Gruppe mit wenigen eindeutigen Apomorphien: Rhinocerotidae. — Paläontologische Zeitschrift, **55**:117–123, Stuttgart.

Heissig, K., 1989. The Rhinocerotidae. — [in:] Prothero, D.R. & Schoch, R.M. (eds.). The evolution of Perissodactyls. — Oxford Monographs on Geology and Geophysics, **15**:399–417, Oxford (Oxford University Press).

Heissig, K., 1996 The stratigraphical range of fossil rhinoceroses in the Late Neogene of Europe and Eastern Mediterranean. — [in:] Bernor, R.L., Fahlbush, V. & Mittman, H.-W., (eds.). The Evolution of Western Eurasian Neogene Mammal Faunas. — 339–347, New York (Columbia University Press).

Hernesniemi, E., Giaourtsakis, I.X., Evans, A.R., & Fortelius, M., (in press). Fossil Rhinoceroses of Laetoli, Tanzania. — [in:] Harrison, T. (ed.). Paleontology and Geology of Laetoli, Tanzania: human evolution in context. Volume 2: Fossil hominins and the associated fauna. — Dordrecht – Berlin – Heidelberg – New York (Springer).

Hsieh, H.-M., Huang, L.-H., Tsai, L.-C., Kuo, Y.-C., Menga, H.-H., Linacre, A. and Lee, C.-I, 2003. Species identification of rhinoceros horns using the cytochrome b gene. — Forensic Science International, **136**:1–11.

Kaup, J., 1832. Über *Rhinoceros incisivus* Cuv., und eine neue Art, *Rhinoceros schleiermacheri.* — Isis von Oken, Jahrgang **1832**(8):898–904, Leipzig

Kaup, J., 1834. Description d'ossements fossiles de mammifères inconnus jusqu'à présent, qui se trouvent au Muséum grand-ducal de Darmstadt. Troisième cahier. — Darmstadt (J.G. Heyer).

Kaya, T., 1994. *Ceratotherium neumayri* (Rhinocerotidae, Mammalia) in the Upper Miocene of Western Anatolia. — Turkish Journal of Earth Sciences, **3**:13–22, Ankara.

Kostopoulos, D.S., Koufos, G.D., Sylvestrou, I.A., Syrides, G.E. & Tsompachidou, E., this volume. The Late Miocene Mammal Faunas of the Mytilinii Basin, Samos Island, Greece: New Collection. 2. Lithostratigraphy and Fossiliferous Sites. — Beiträge zur Paläontologie, **31**:13–26, Wien.

Koufos, G.D., 1980. Paleontological and stratigraphical study of the Neogene continental deposits of Axios Valley (Macedonia, Greece). [in Greek]. — Scientific Annals of the Faculty of Physics and Mathematics, Aristotelian Univercity of Thessaloniki, **19**:1–322, Thessaloniki.

Koufos, G.D., this volume. The Late Miocene Mammal Faunas of the Mytilinii Basin, Samos Island, Greece: New Collection. 1. History of the Samos Fossil Mammals. — Beiträge zur Paläontologie, **31**:1–12, Wien.

Koufos, G.D., Kostopoulos, D.S. & Vlachou, D., this volume-a. The Late Miocene Mammal Faunas of the Mytilinii Basin, Samos Island, Greece: New Collection. 16. Chronology. — Beiträge zur Paläontologie, **31**:397–408, Wien.

Koufos, G.D., Kostopoulos, D.S. & Merceron, G., this volume-b. The Late Miocene Mammal Faunas of the Mytilinii Basin, Samos Island, Greece: New Collection. 17. Palaeoecology - Palaeobiogeography. — Beiträge zur Paläontologie, **31**:409–430, Wien.

Kretzoi, M., 1942. Bemerkungen zum System der nachmiozänen Nashorn-Gattungen. — Földtani Közlöny, **72**:309–318, Budapest.

Leader-Williams, N. 1985. Black rhino in South Luangwa National Park: their distribution and future protection. — Oryx, **19**:27–33, London.

Lehmann, U., 1984. Notiz über Säugetierreste von der Insel Samos in der Sammlung des Geologisch-Paläontologischen Instituts und Museums Hamburg. — Mitteilungen aus dem Geologischen-Paläontologischen Institut der Universität Hamburg, **57**:147–156, Hamburg,

Leonardi, P., 1947. Resti fossili inediti di rinoceronti conservati nelle collezioni dell' Istituto Geologico dell' Università di Padova. — Memorie dell'Instituto Geologico dell'Università di Padova, **15**:3–30, Padova.

Loose, H. 1975. Pleistocene Rhinocerotidae of W. Europe with reference to the recent two-horned species of Africa and S. E. Asia. — Scripta Geologica, **33**:1–59, Leiden.

Loutit, B.D., Louw, G.N. & Seely, M.K., 1987. First approximation of food preference and the chemical composition of the diet of the desert-dwelling black rhinoceros (*Diceros bicornis*). — Madoqua, **15**:35–54, Windhoek.

McKenna, M.C. & Bell, S.K., 1997. Classification of mammals above the species level. — pp. 631, New York (Columbia University Press).

Mecquenem, R. de, 1924. Contribution à l'étude des fossiles de Maragha. — Annales de Paléontologie, **13**:135–160, Paris.

Meiburg, P. & Siegfried, P. 1970. Katalog der Typen und Belegstücke zur Paläozoologie im Geologisch-Paläontologischen Institut der Westfälischen Wilhelms-Universität Münster. II. Teil: Vertebrata. — Münstersche Forschungen zur Geologie und Paläontologie, **15**:1–84, Münster.

Melentis, J.K., 1967. Die Pikermifauna von Halmyropotamos (Euboea - Griechenland) 1. Teil: Odontologie und Craniologie. — Annales Géologiques des Pays Helléniques, **19**:83–341, Athens.

Melentis, J.K., 1968. Palaeontological excavations at Samos Island, a preliminary report [in Greek]. — Proceedings of the Academy of Athens, **43**:344–349, Athens.

Melentis, J.K., 1969. Die Pikermifauna von Halmyropotamos (Euboea - Griechenland) 2. Teil: Osteologie. — Annales Géologiques des Pays Helléniques, **21**:217–306, Athens.

Morales, J.C. & Melnick, D.J. 1994. Molecular systematics of the living rhinoceros. — Molecular Phylogenetics and Evolution, **3**:128–134, Orlando.

NAV, 2005: Nomina Anatomica Veterinaria, 5th edition. — International Committee on Veterinary Gross Anatomical Nomenclature, pp. 166, Hannover-Columbia-Genf-Sapporo.

Oloo, T.W., Brett, R. & Young, T.P., 1994. Seasonal variation in the feeding ecology of black rhinoceros (Diceros bicornis) in Laikipia, Kenya. — African Journal of Ecology, **32**:142–157, Oxford.

Orlando, L., Leonard, J.A., Thenot, A., Laudet, V., Guérin, C. & Hänni, C., 2003. Ancient DNA analysis reveals woolly rhino evolutionary relationships. — Molecular Phylogenetics and Evolution, **28**:485–499, Orlando.

Osborn, H.F., 1900. Phylogeny of the rhinoceroses of Europe. — Bulletin of the American Museum of

Natural History, **12**:229–267, New York.

Pavlow, M.W., 1913. Mammifères tertiaires de la Nouvelle Russie, 1. Partie: Artiodactyla, Perissodactyla (Aceratherium kowalevskii n.s.). — Nouveaux Mémoires de la Société Impériale des Naturalistes de Moscou, **17**:1–68, Moscow.

Peter, K., 2002. Odontologie der Nashornverwandten (Rhinocerotidae) aus dem Miozän (MN 5) von Sandelzhausen (Bayern). — Zitteliana, **22**:3–168, München.

Pethő, G., 1884. Über die Fossilien Säugethier-Überreste von Baltavár. — Földtani Intézet Évi Jelentése, **1884**:63–73, Budapest.

Piccolo, G., Franco, F., Bertolotti, O., Bimbatti, M., Buja, P., Cesga, L. & Gradenico, M., 1975. I resti di mammiferi del Neogene di Samos e Pikermi (Grecia) conservationel museo geologico e paleontologico dell'università di Padova. — Memorie degli Istituti di Geologia e Mineralogia dell'Università di Padova, **31**:1–39, Padova.

Prothero, D.R., Manning, E. & Hanson, B.C., 1986. The phylogeny of the Rhinocerotoidea (Mammalia, Perissodactyla). — Zoological Journal of the Linnean Society, **87**:341–366, London.

Prothero, D.R. & Schoch, R.M., 1989. Classification of the Perissodactyla. — [in:] Prothero, D.R. & Schoch, R.M (eds.). The evolution of Perissodactyls. — Oxford Monographs on Geology and Geophysics, 15:530–537, Oxford (Oxford University Press).

Ringström, T., 1924. Nashörner der Hipparion-Fauna Nord-Chinas. — Palaeontologia Sinica, C, **1**(4):1–156, Beijing.

Roth, J. & Wagner, A., 1854. Die fossilen Knochenüberreste von Pikermi in Griechenland. — Abhandlungen der Bayerischen Akademie der Wissenschaften, **7**:371–464, München.

Ruspoli, M. 1987. The Cave of Lascaux: The Final Photographic Record — pp. 206, London (Thames and Hudson).

Schlosser, M., 1921. Die Hipparionenfauna von Veles in Mazedonien. — Abhandlungen der Bayerischen Akademie der Wissenschaften, **29**(4):1–55, München.

Solounias, N., 1981a. The Turolian fauna from the Island of Samos, Greece - with special emphasis on the hyaenids and the bovids. — Contributions to Vertebrate Evolution, **6**:1–232, Basel.

Solounias, N., 1981b. Mammalian fossils of Samos and Pikermi. Part 2. Resurrection of a classic Turolian fauna. — Annals of the Carnegie Museum, **50**:231–270, Pittsburgh.

Solounias, N. & Mayor, A., 2004. Ancient references to the fossils from the land of Pythagoras. — Earth Sciences History, **23**(4):283–296, New York.

Thenius, E., 1955. Zur Kenntnis der unterpliozänen Diceros-Arten. — Annalen des Naturhistorischen Museums in Wien, **60**:202–209, Wien.

Thenius, E., 1956. Über das Vorkommen von *Diceros pachygnathus* (Wagner) im Pannon (Unter-Pliozaen) des Wiener Beckens. — Neues Jahrbuch für Geologie und Palaeontologie, Monatshefte, **1**:35–39, Stuttgart.

Tong, H. 2000. Les Rhinocéros de sites à fossiles humains de Chine. — L'Anthropologie, **104**:523–529, Paris.

Toula, F., 1906. Das Gebiss und Reste der Nasenbeine von *Rhinoceros* (*Ceratorhinus* Osborn) *hundsheimensis*. — Abhandlungen der k.k. Geologischen Reichsanstalt, Wien, **20**(2):1–38, Wien.

Tougard, C., Delefosse, T., Hänni, C. & Montgelard, C., 2001. Phylogenetic Relationships of the Five Extant Rhinoceros Species (Rhinocerotidae, Perissodactyla) based on Mitochondrial Cytochrome b and 12S rRNA Genes. — Molecular Phylogenetics and Evolution, **19**:34–44, Orlando.

Tsiskarishvili, G.V., 1987. Pozdnetvetichnye nosorogi (Rhinocerotidae) Kavkaza - Late Tertiary rhinoceroses (Rhinocerotidae) of the Caucasus [in Russian]. — GruzSSR, Gosudarstvennyy Muzey Gruzii, Izdatel'stvo Metsnierba, — pp. 141, Tbilisi.

Viret, J., 1958. Perissodactyla. — [in:] Piveteau, J. (ed.). Traité de Paléontologie. — **4**:368–475, Paris (Masson).

Wagner, A., 1848. Urweltliche Säugetiere-Überreste aus Griechenland. — Abhandlungen der Bayerischen Akademie der Wissenschaften, **5**:335–378, München.

Weber, M., 1904. Über tertiäre Rhinocerotiden von der Insel Samos I. — Bulletin de la Société Impériale des Naturalistes de Moscou, **17**:477–501, Moscow.

Weber, M., 1905. Über tertiäre Rhinocerotiden von der Insel Samos II. — Bulletin de la Société Imperériale des Naturalistes de Moscou, **18**:345–363, Moscow.

Zeuner F. 1934. Die Beziehungen zwischen Schädelform und Lebensweise bei den rezenten und fossilen Nashörnern. — Berichte der Naturforschenden Gesellschaft zu Freiburg, **34**:21–79, Freiburg.

PLATE 1

Fig. 1. "*Diceros*" *neumayri* (Osborn, 1900) from Mytilinii Basin, Samos, Greece. Adult cranium (NHMA: MTLA-5) in left lateral view. Note that the zygomatic arch is deformed and mediodorsally elevated, due to postmortem fraction and rotation. Scale bar 10 cm.

Fig. 2a. "*Diceros*" *neumayri* (Osborn, 1900) from Mytilinii Basin, Samos, Greece. Adult cranium (NHMA: PMMS-107) in left lateral view. Scale bar 10 cm.

Fig. 2b. Same specimen in dorsal view. Scale bar 10 cm.

PLATE 1

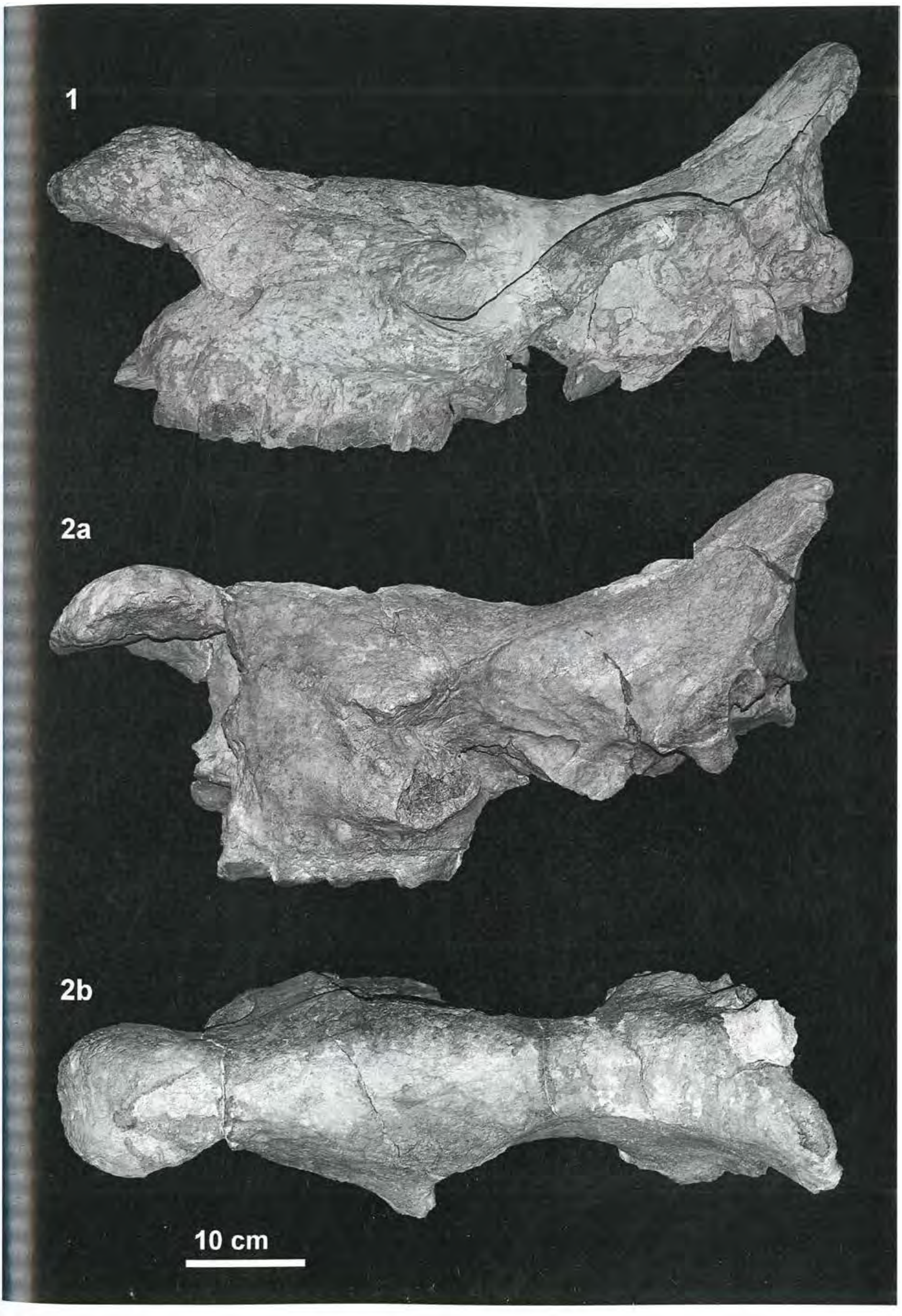

PLATE 2

Fig. 1. "*Diceros*" *neumayri* (Osborn, 1900) from Mytilinii Basin, Samos, Greece. Adult cranium (NHMA: MTLA-5) in ventral view. Scale bar 10 cm.

Fig. 2a. "*Diceros*" *neumayri* (Osborn, 1900) from Mytilinii Basin, Samos, Greece. Juvenile cranium (NHMA: MTLA-212) in left lateral view. Scale bar 10 cm.

Fig. 2b. Same specimen in dorsal view. Scale bar 10 cm.

PLATE 2

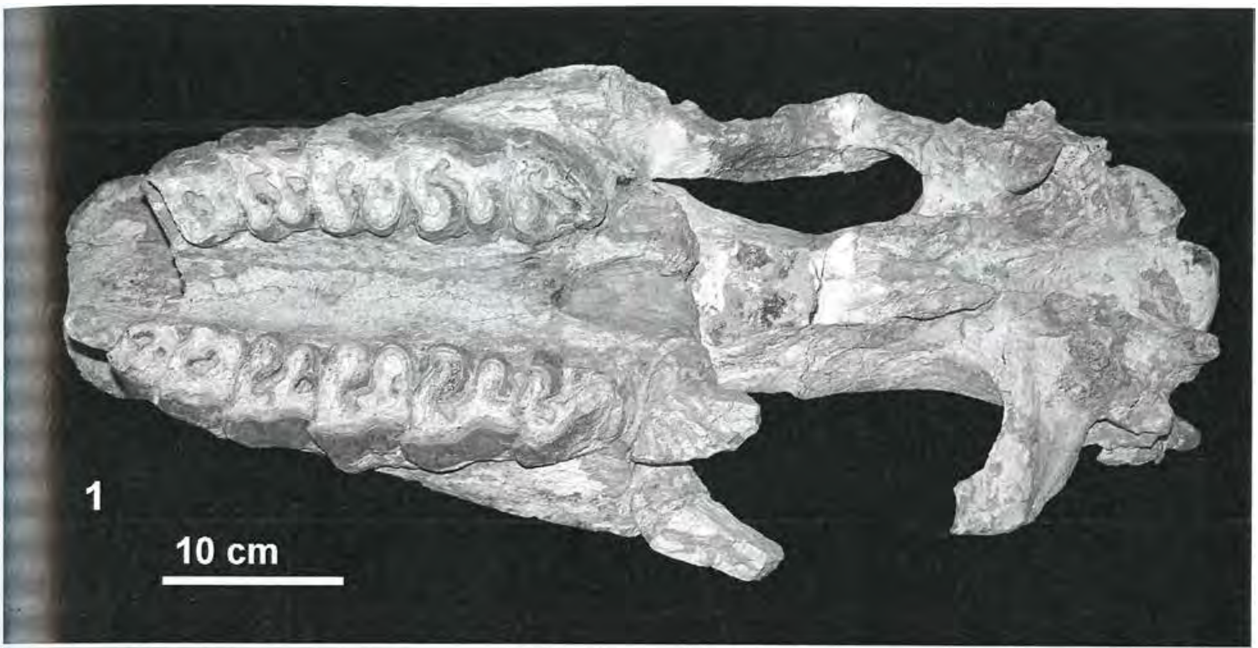

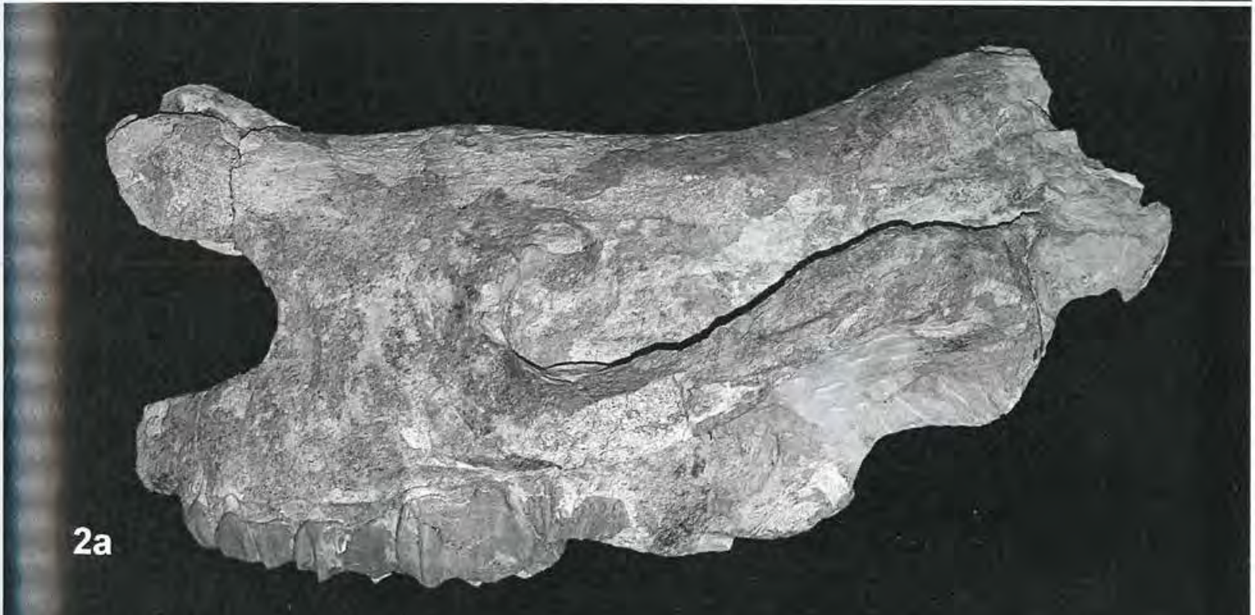

PLATE 3

Fig. 1. *"Diceros" neumayri* (Osborn, 1900) from Mytilinii Basin, Samos, Greece. Adult mandible (NHMA: PMMS-106) in right lateral view. Scale bar 10 cm.

Fig. 2a. *"Diceros" neumayri* (Osborn, 1900), from Mytilinii Basin, Samos, Greece. Adult mandible (NHMA: PMMS-108) in left lateral view (reversed image). Scale bar 10 cm.

Fig. 2b. Same specimen in dorsal view. Scale bar 10 cm.

Fig. 2c. Same specimen, detail of the mandibular symphysis in oblique rostral view. Arrow indicates the presence of a sagittal crest on the ventral surface of the mandibular symphysis. Not in scale.

Fig. 3. *Dihoplus pikermiensis* (Toula, 1906) from Mytilinii Basin, Samos, Greece. Right Mt-III (NHMA: MYT-65) in proximal view. Arrow indicates the presence of a small articular facet for the cuboid. Also note the presence of an indentation on the dorsal border of the articular facet for the ectocuneiform. Scale bar 2 cm.

Fig. 4. *Dihoplus pikermiensis* (Toula, 1906) from Pikermi, Attica, Greece. Right Mt-III (BMNH: M.11317) in proximal view. Arrow indicates the presence of an articular facet for the cuboid, better developed in this individual. Also note the presence of an indentation on the dorsal border of the articular facet for the ectocuneiform. Scale bar 2 cm.

Fig. 5. *"Diceros" neumayri* (Osborn, 1900), from Mytilinii Basin, Samos, Greece. Right Mt-III (NHMA: MTLB-21) in distal view. Arrow indicates the sagittal keel of the articular head, which is weakly developed and remains below the level of the medial rim. Scale bar 2 cm.

Fig. 6. *Dihoplus pikermiensis* (Toula, 1906) from Pikermi, Attica, Greece. Right Mt-III (BMNH: M.48161) in distal view. Note that the sagittal keel is sharper and more prominent, surpassing the level of the medial rim of the articular head. Scale bar 2 cm.

PLATE 3

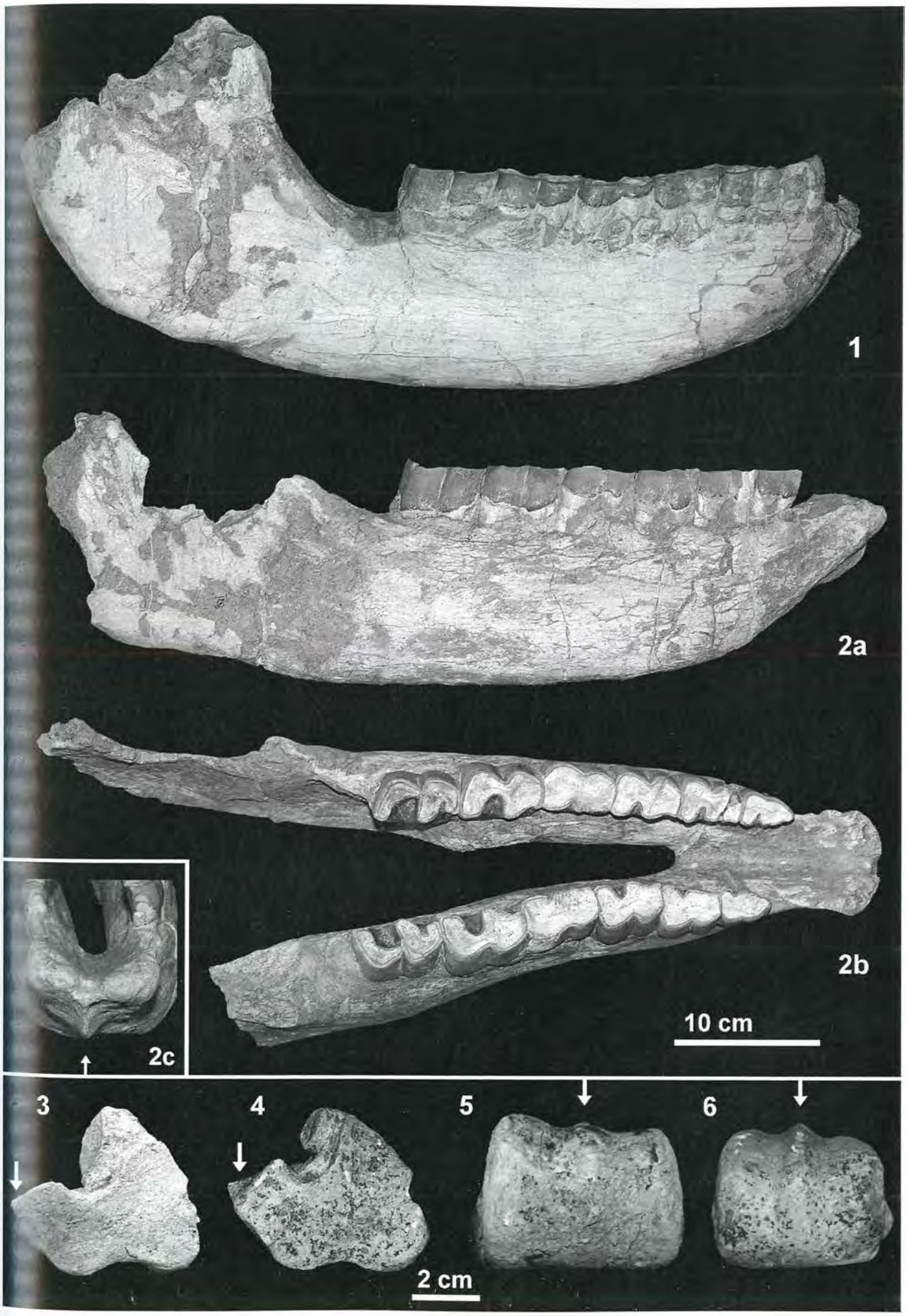

PLATE 4

Fig. 1. *"Diceros" neumayri* (Osborn, 1900), from Mytilinii Basin, Samos, Greece. Right upper dentition, P2-M3, of the adult cranium (NHMA: MTLA-5) in occlusal view. Scale bar 5 cm.

Fig. 2. *"Diceros" neumayri* (Osborn, 1900), from Mytilinii Basin, Samos, Greece. Adult maxillary fragment with right upper M2-M3 (NHMA: MTLA-425) in occlusal view. Scale bar 5 cm.

Fig. 3. *"Diceros" neumayri* (Osborn, 1900), from Mytilinii Basin, Samos, Greece. Left upper dentition, P4-M3, of the adult cranium (NHMA: PMMS-107) in occlusal view. Scale bar 5 cm.

Fig. 4. *"Diceros" neumayri* (Osborn, 1900), from Mytilinii Basin, Samos, Greece. Left lower dentition, p2-m3, of the adult mandible (NHMA: PMMS-108) in occlusal view. Scale bar 5 cm.

Fig. 5. *"Diceros" neumayri* (Osborn, 1900), from Mytilinii Basin, Samos, Greece. Right lower dentition, p2-m3, of the adult mandible (NHMA: PMMS-106) in occlusal view. Scale bar 5 cm.

Fig. 6. *"Diceros" neumayri* (Osborn, 1900), from Mytilinii Basin, Samos, Greece. Left upper deciduous dentition, D1-D4, of the juvenile cranium (NHMA: MTLA-212) in occlusal view. Scale bar 5 cm.

Fig. 7. *"Diceros" neumayri* (Osborn, 1900), from Mytilinii Basin, Samos, Greece. Right lower deciduous dentition with d1 and d3-d4 (NHMA: MTLA-179) in occlusal view. On d3, a closed paralophid groove is formed, but the small fossettid is filled with sediment. Scale bar 4 cm.

Fig. 8. *"Diceros" neumayri* (Osborn, 1900), from Mytilinii Basin, Samos, Greece. Right lower deciduous dentition with d1-d4 (HLMD: SS-77) in occlusal view. Note the closed talonid basin on d2 (fossettid indicated by letter T), and the presence of a closed paralophid groove on d3 (small fossettid indicated by letter P). Scale bar 4 cm.

Fig. 9. *"Diceros" neumayri* (Osborn, 1900), from Mytilinii Basin, Samos, Greece. Right lower deciduous dentition with d1-d4 (NHMW: 1911-V.44) in occlusal view. Note the worn fossettid of the closed talonid basin of d2. On d3, the two paralophid lobes have fused, obliterating the paralophid groove. Scale bar 4 cm.

Fig. 10. *"Diceros" neumayri* (Osborn, 1900), from Mytilinii Basin, Samos, Greece. Right lower deciduous dentition with d3-d4 (BMNH: M.4396) in occlusal view. Note that the two paralophid lobes on d3 are separated and the paralophid groove is open. Scale bar 4 cm.

PLATE 4

1

2

3

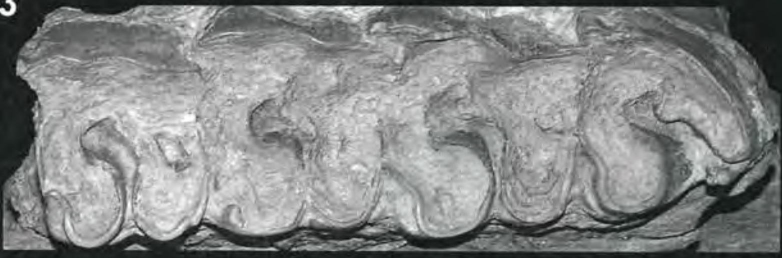

6

7

8

9

10

4

5

PLATE 5

Fig. 1. *Dihoplus pikermiensis* (Toula, 1906) from Pikermi, Attica, Greece. Left Mc-III (AMNH: ΠA-601) in dorsal view. Scale bar 4 cm.

Fig. 2. *Dihoplus pikermiensis* (Toula, 1906) from Mytilinii Basin, Samos, Greece. Associated right metacarpals (NHMA: MYT-48) in dorsal view; Mc-IV (2a), Mc-III (2b), and Mc-II (2c). Scale bar 4 cm.

Fig. 3. *"Diceros" neumayri* (Osborn, 1900), from Mahmutgazi, Turkey. Right Mc-II (SMNK: Ma1-Nr.98) in dorsal view. Scale bar 4 cm.

Fig. 4. *"Diceros" neumayri* (Osborn, 1900), from Mytilinii Basin, Samos, Greece. Left Mc-III (NHMW: 1911-V.340) in dorsal view. Note the markedly concave lateral margin of the diaphysis. Scale bar 4 cm.

Fig. 5. *"Diceros" neumayri* (Osborn, 1900), from Pikermi, Attica, Greece. Right Mc-III (MNHN: PIK-1010d) in dorsal view. Arrow indicates the markedly concave lateral margin of the diaphysis. Scale bar 4 cm.

Fig. 6. *"Diceros" neumayri* (Osborn, 1900), from Mahmutgazi, Turkey. Right Mc-III (SMNK: Ma1-Nr.94) in dorsal view. Note the markedly concave lateral margin of the diaphysis. Scale bar 4 cm.

Fig. 7. *"Diceros" neumayri* (Osborn, 1900), from Mahmutgazi, Turkey. Left Mc-IV (SMNK: Ma1-Nr.98) in dorsal view. Arrow indicates the relatively short but strong rugosity for the attachment of the interosseous ligament. Scale bar 4 cm.

Fig. 8a. *Dihoplus pikermiensis* (Toula, 1906) from Mytilinii Basin, Samos, Greece. Right astragalus (NHMA: MTLD-8) in plantar view. Note the large sustentacular calcaneal facet with an irregular subcircular outline. This facet merges distolaterally with the distal calcaneal facet, but has no direct contact with the articular facet for the cuboid. Scale bar 4 cm.

Fig. 8b. Same specimen in lateral view. Note that the bowed articular stripe for the lateral malleolus of the fibula has a rather constant width throughout its length, and establishes a wide contact with the ectal facet for the calcaneus. The attachment surface for the lateral talocalcaneal ligament is relatively small. Scale bar 4 cm.

Fig. 9a. *"Diceros" neumayri* (Osborn, 1900), from Mytilinii Basin, Samos, Greece. Left astragalus (NHMW: unnumbered) in plantar view (reversed image). Note the high-oval outline of the sustentacular calcaneal facet. There is a contact with the cuboid facet, but not with the distal calcaneal facet. Scale bar 4 cm.

Fig. 9b. Same specimen in lateral view (reversed image). Note that the width of the bowed fibular stripe reduces gradually towards its proximal tip and has no contact with the ectal facet for the calcaneus. The attachment surface for the lateral talocalcaneal ligament is more extensive. Scale bar 4 cm.

Fig. 10. *"Diceros" neumayri* (Osborn, 1900) from Mytilinii Basin, Samos, Greece. Adult cranium (NHMA: MTLA-5) in occipital view. Scale bar 10 cm.

PLATE 5